Chapter-4

EXPERIMENTAL RESULTS

The results of the present experiment are obtained by using the new data acquisition system (section 2.1 of chapter 2) of the NBU EAS telescope. The search for UHE discrete point sources is now the thrust of the investigation using NBU EAS telescope. At the first phase of investigation in this direction, a set of 14,260 shower events were analysed during the period of January '95 to July '96 detected in the size range $2X10^4$ - $3X10^6$ particles. Total observation time is ~985 hours. The results presented are from those showers which have zenith angle $\leq 60^o$ and chi-square per degree of freedom less than 5, because above $\chi^2=5$,the observed data were not in good fit to the fitting function. For the same reason, showers with age parameter greater than 1.8 and less than 0.6 were also rejected. Percentage of shower events rejected due to different causes are shown in table-1.

Table-1

Sl. No.	Cause of rejection	Rejected showers in percent
1.	Spurious coincidence (see option-1 & 3, section-3.1.1., chapter-3).	~0.1%
2.	Zenith angle > 60^o.	~ 5%
3.	χ^2 >5	~ 8%
4.	Shower age (s) <0.6 and s >1.8	~ 10%

Table-1: Rejection of shower events in percent.

For the observation of gamma ray sources, it is necessary to check the behaviour of the shower characteristics. If any systematic bias is involved in the measurement of shower parameters and angular directions, it will surely reflect on the general characteristics of the observed air shower. So, to make sure that there is no

systematic errors, the general characteristics of air shower are described in two sections. In the first section-4.1, fundamental properties of EAS are presented. In the second section-4.2, the results of the study carried out on shower age parameter, are presented.

4.1 **Fundamental properties of EAS:**

4.1.1 **Lateral distribution of electrons(LDE) in EAS :**

The lateral distribution of electrons (LDE) is important as a basic parameter of an EAS for the accurate determination of the total number of electrons in the shower i,e electron shower size (N_e).

In order to construct the average lateral distribution , all showers with zenith angle $\leq 60^o$ are divided into groups with two narrow size bins (7-9)X10^4 and (8-10)X10^5. Each shower size bin is then again subdivided into three zenith angle bins (0^o-20^o), (20^o-40^o), (40^o-60^o) and for each subgroup, whole radial distance is divided into narrow intervals. For a particular value of shower age(s), the average density and average radial distance at a given radial distance interval was calculated by-

$$\Delta(r) = \Sigma \Delta(r)_i/n$$
$$r = \Sigma r_i/n$$

where n is the number of showers in that interval.The average shower size for every shower size bin are then calculated.

The average lateral distribution of electrons so constructed for the two shower sizes with three different zenith angle bins along with the Hillas distribution function are shown in fig. 4.1a, 4.1b and 4.1c. From the fig.4.1a. or 4.1b. or fig.4.1c., it is observed that the structure of the lateral distribution of electrons is independent for different shower sizes for a given zenith angle range.

Again fig.4.1d shows that the structure of the lateral distribution of electrons is independent for different zenith angle ranges for a given shower size.

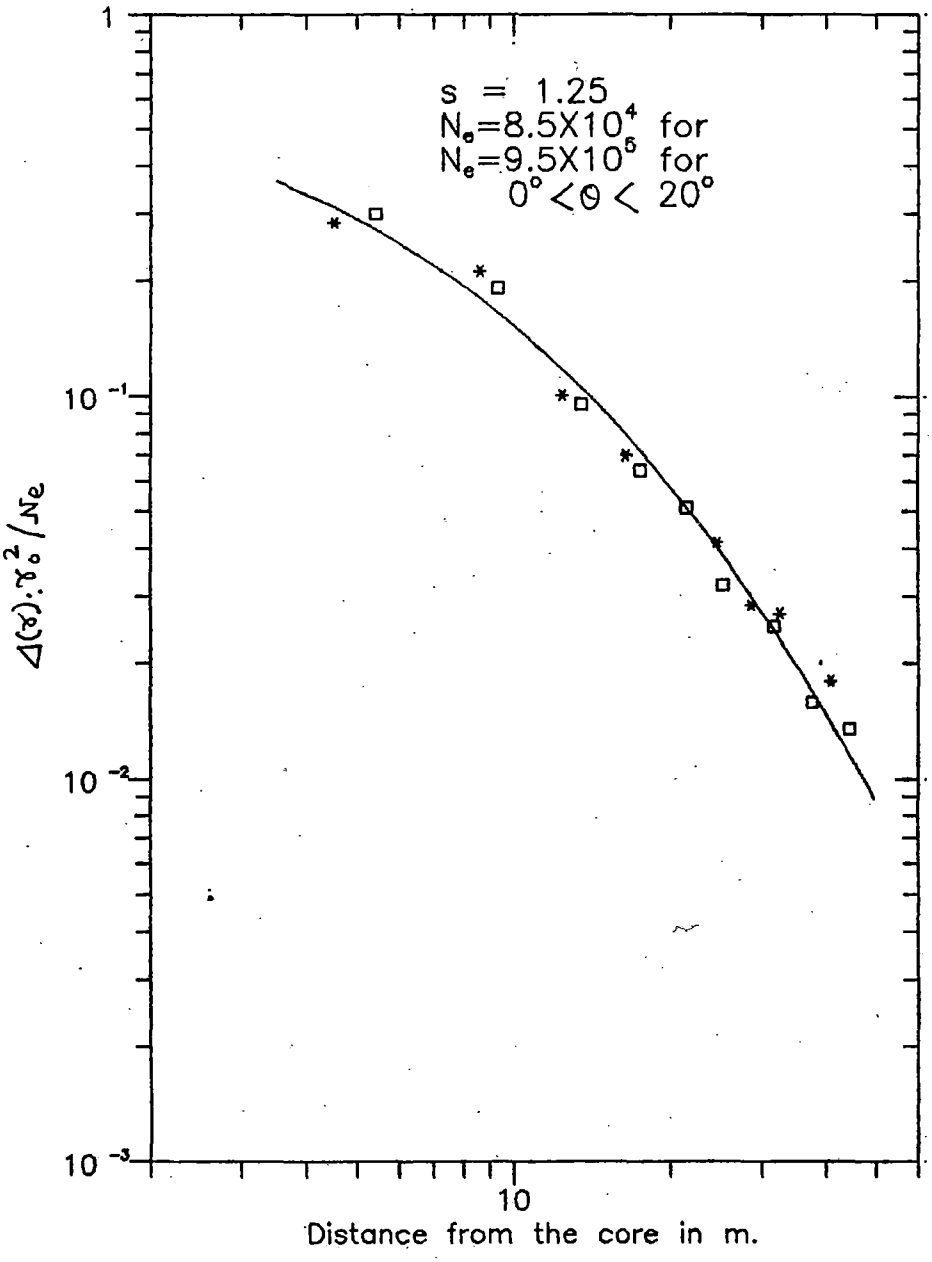

Fig.4.1a.
Lateral distribution of Electrons compared with Hillas distribution function.

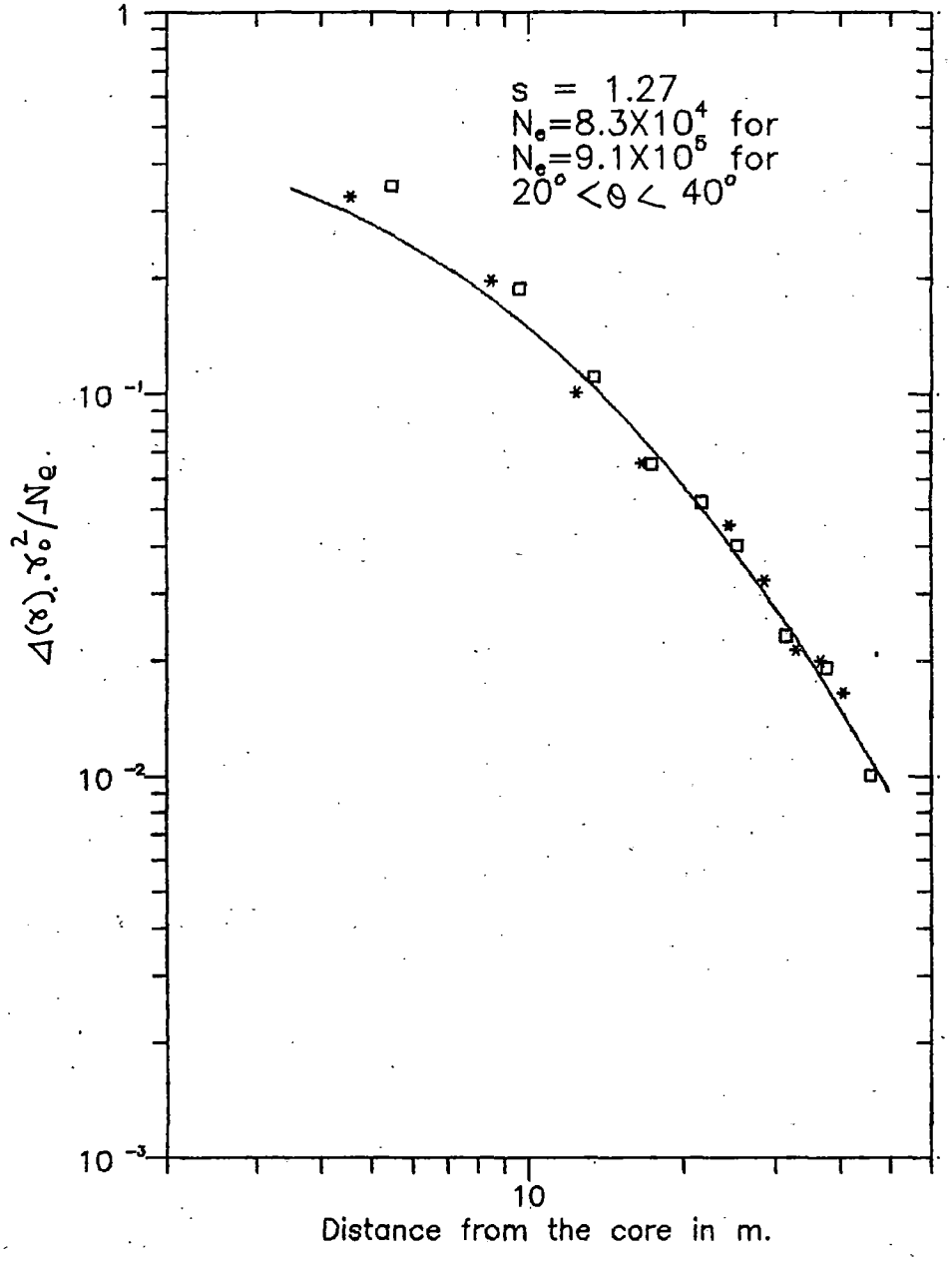

Fig.4.1b.
Lateral distribution of
Electrons compared with
Hillas distribution function.

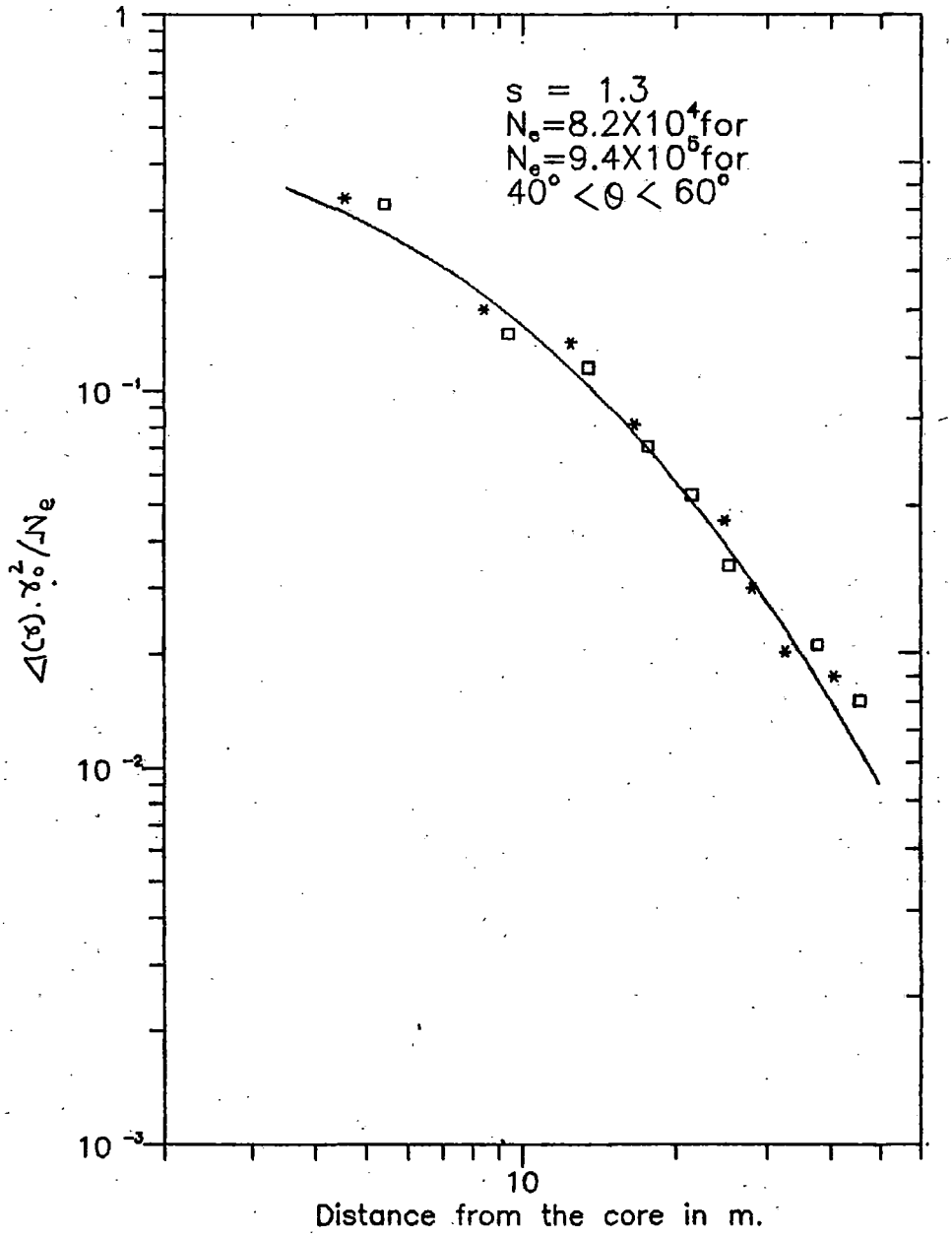

Fig.4.1c.
Lateral distribution of Electrons compared with Hillas distribution function.

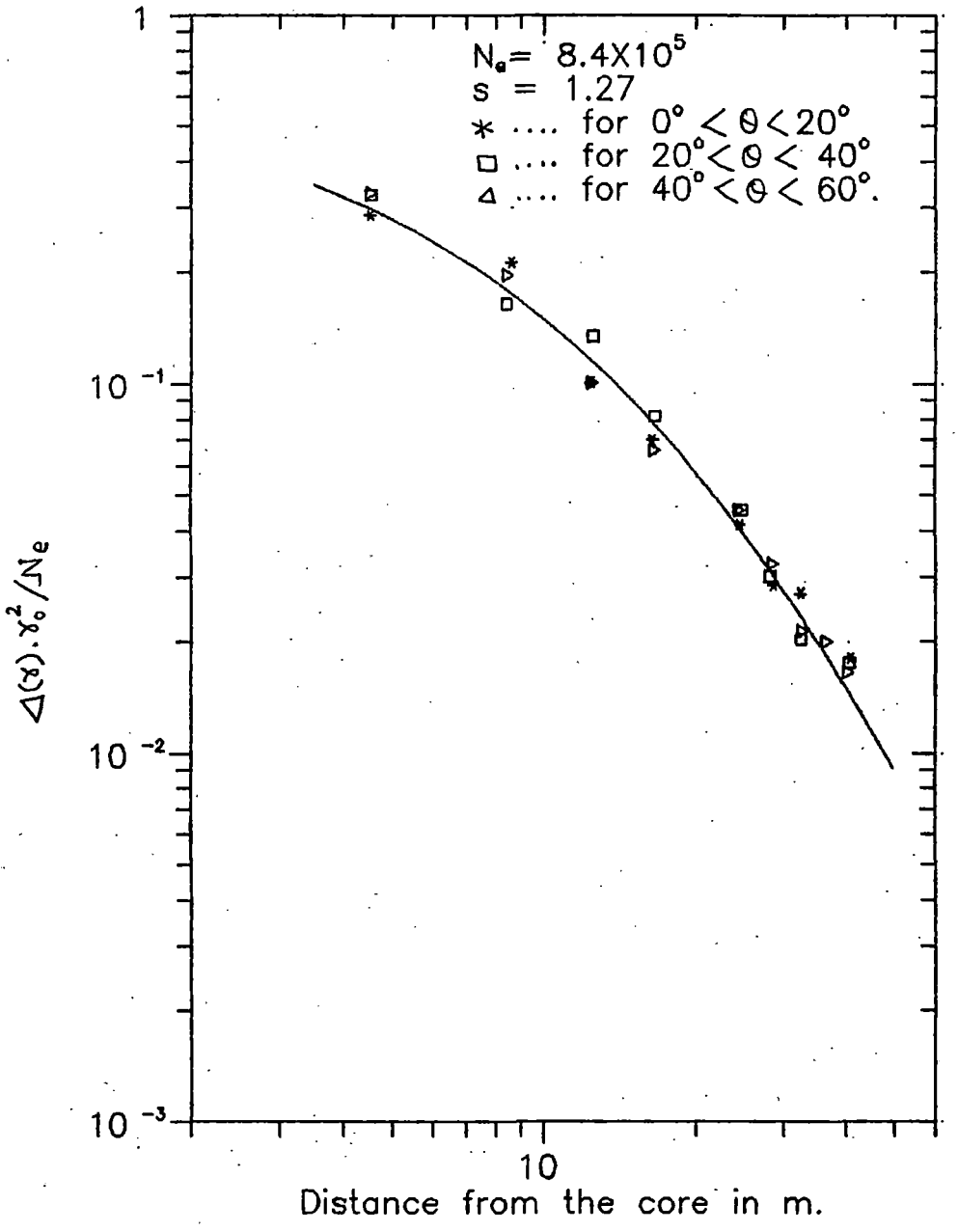

Fig.4.1d.
Lateral distribution of Electrons for a given size with different zenith angle.

A comparison of lateral distribution of electrons for the shower size bin (2-3)X10^5 with the experimental results of Catz (Catz Ph et al.[1]) at the same observation level is shown in fig.4.1e. The result is in satisfactory agreement with the result of Catz .

4.1.2 **Shower size distribution and shower age distribution :**

Shower size distribution:

Distribution of shower size in the size range 2X10^4-3X10^6 detected by the NBU telescope is shown in fig.4.1f. From the distribution it is seen that the shower size at the highest frequency is in the range (1-2)X10^5 particles.

Shower age distribution:

The shower 'age' (s) determined by the χ^2-minimisation of Hillas lateral distribution function indicates quantitatively how peaked or how flat the lateral distribution of electron density is with respect to the shower axis direction. The distribution of age parameter of the observed shower events is shown in fig.4.1g. The observed shower age distribution is found to be a Gaussian distribution with mean value 1.39 and standard deviation 0.19. At the same observation level and with primary particle energy > 5X10^{14} eV, experimental age distribution obtained by Haverah Park array (Idenden D.W.[2]) is also Gaussian with mean value 1.45. The present mean value of the age distribution is in aggrement with the theoretical estimation 1.33 of Fenyves (Fenyves J.[3]) for proton initiated showers with primary energy ~10^{15} eV at the same observation level within the experimental uncertainties.
From the shower age distribution, it is observed that~3.6% of showers are detected with values of shower age in the range $0.6 \leq s < 1$. This is due to the developmental fluctuation of EAS in the atmosphere.

4.1.3. **Angular distribution of observed EAS :**

Zenith angle distribution :

The zenith angle distribution has been measured for many years , either deliberately to study the physics of shower development or to check the array performance. Zenith angle and azimuth angle of incident EAS are determined by the usual first

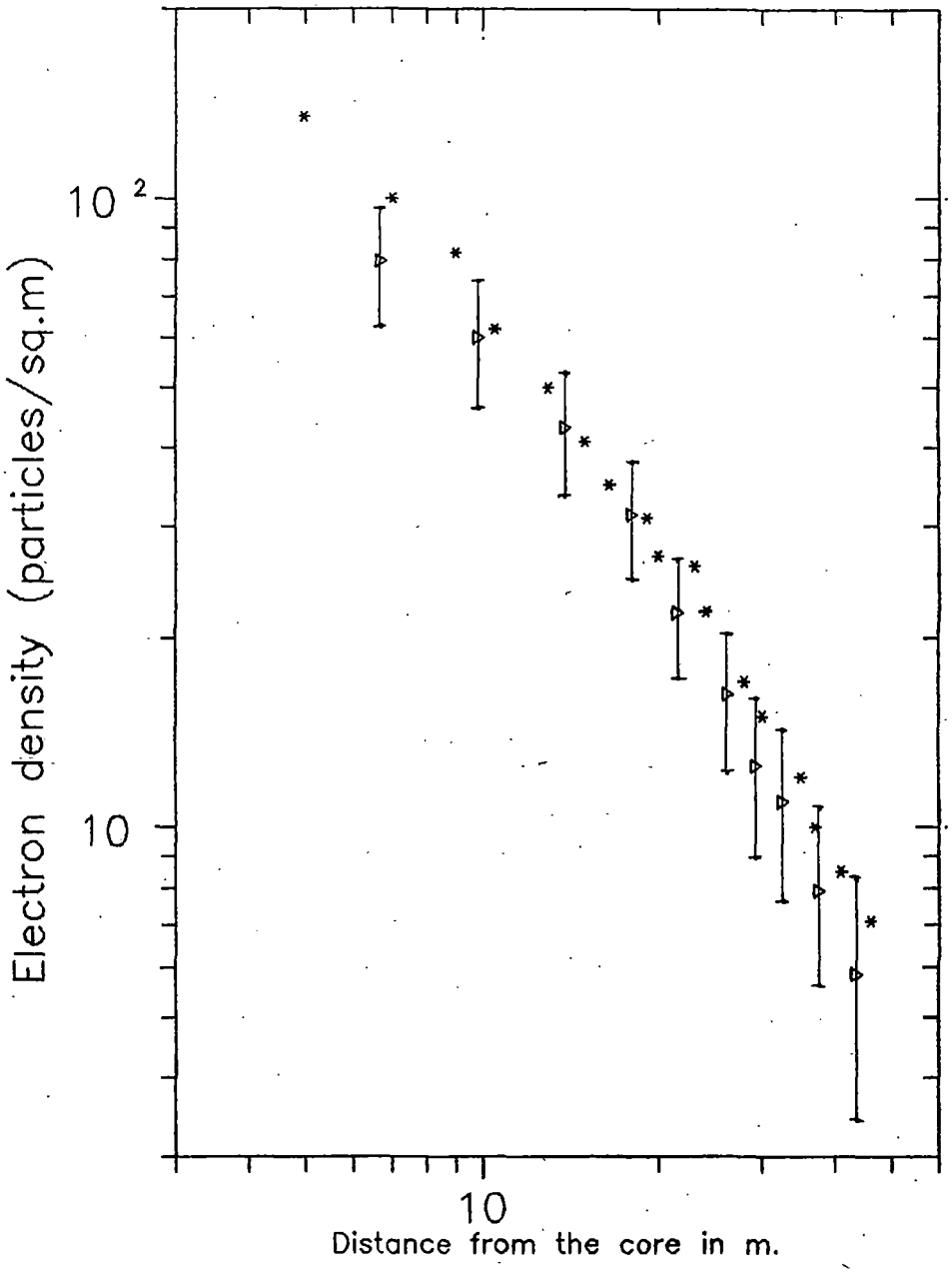

Fig.4.1e.
Experimental lateral distribution of Electrons compared with experimental result of Catz et al.
Catz et al.*, $N_e=3X10^5$, S=1.25
Present expt. Δ , $N_e=2.4X10^5$, s=1.27

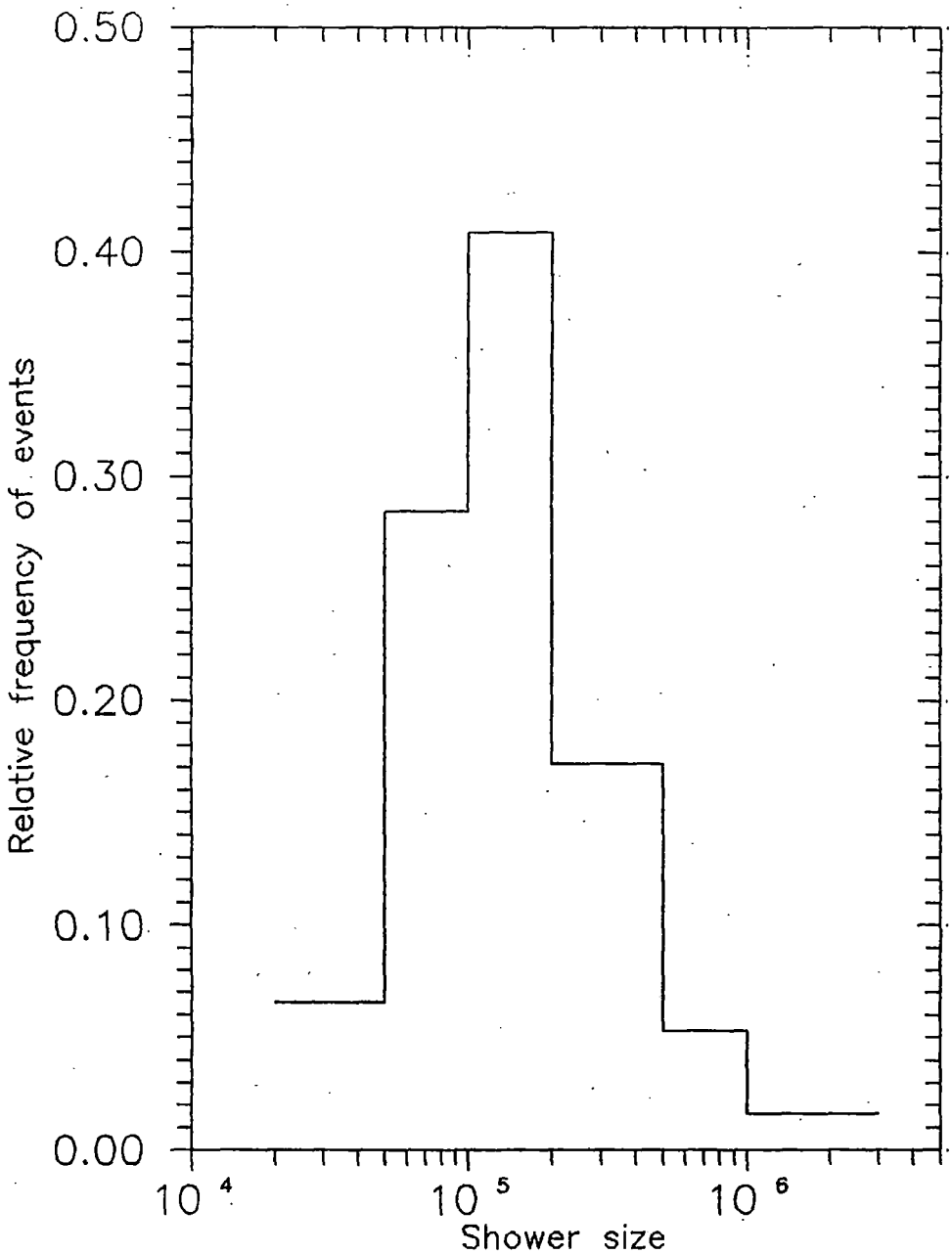

Fig.4.1f.
Shower size distribution of the observed shower events.

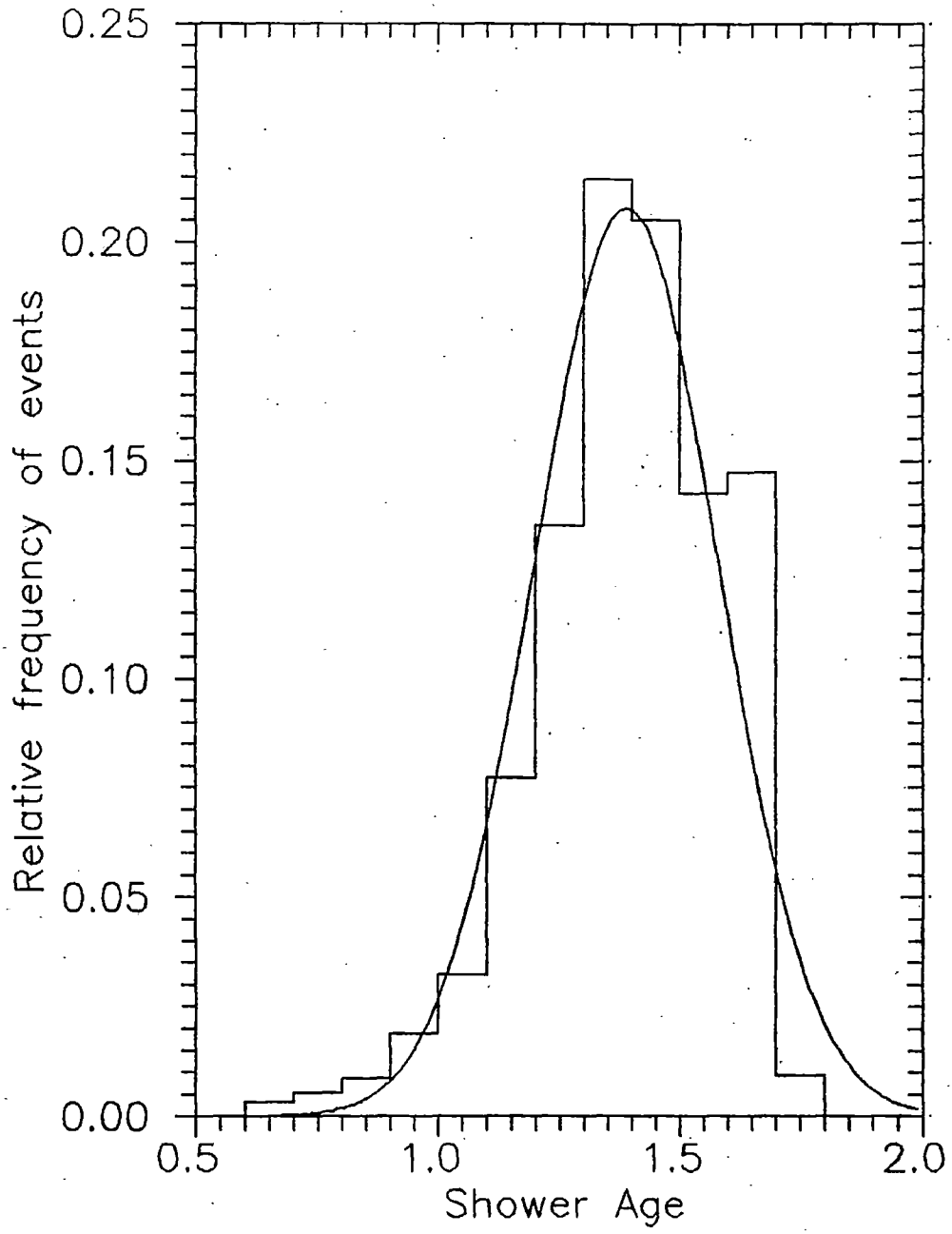

Fig.4.1g.
Distribution of shower age
of the observed shower events.

timing technique as described in the previous chapter. The errors of zenith angle measurements in the present experiment do not exceed 1.15^{o} in an individual EAS. The zenith angle distribution in the interval 0^{o} - 60^{o} for the three shower size ranges (4-9)$X10^{4}$, $9X10^{4}$ - $2X10^{5}$, (2- 5)$X10^{5}$ is shown in fig.4.1h, 4.1i. and 4.1j. From the figures, it is clear that the number of events observed at a given zenith angle bin first increases with zenith angle due to the increase in solid angle , reaches a peak around 18^{o} and then falls at higher zenith angles, because at higher zenith angles the atmospheric absorption part (depending on t.secθ) dominates over the solid angle of acceptance part and as a result the number of events within a zenith angle bin falls.

To remove the solid angle effect of zenith angle distribution, the frequency of events are divided by sinθ. A least square fit to the Ln(Intensity) vs Ln(cosθ)data has been made and fit is shown in fig.4.1k, 4.1l. and 4.1m. Result of the fit is

$$Ln(I) = 6.64 \cos\theta + 5.32 \text{ ; for the size range } (4\text{-}9)X10^{4}$$

$$Ln(I) = 7.45 \cos\theta + 5.94 \text{ ; for the size range } 9X10^{4}\text{-}2X10^{5}$$

$$Ln(I) = 8.77 \cos\theta + 5.43 \text{ ; for the size range } (2\text{-}5)X10^{5}$$

From the fit, it is clear that , the value of the power index increases with the increase of shower size.

To check the consistency of the zenith angle distribution for the above three size ranges, frequency of events are divided by sinθ and plotted against secθ as shown in fig 4.1n, 4.1o. and 4.1p. This gives almost linear relationship up to $\theta \simeq 40^{o}$ as-

$$Log (I) = -3.25.\sec\theta + 5.61 \text{ ; for the size range } (4\text{-}9)X10^{4}$$

$$Log (I) = -3.35.\sec\theta + 5.96 \text{ ; for the size range } 9X10^{4}\text{-}2X10^{5}$$

$$Log (I) = -3.46.\sec\theta + 5.82 \text{ ; for the size range } (2\text{-}5)X10^{5}$$

Here also the slope of the curves increases with the increase of shower size. In the same observation level and zenith angle range with different triggering thresholds,

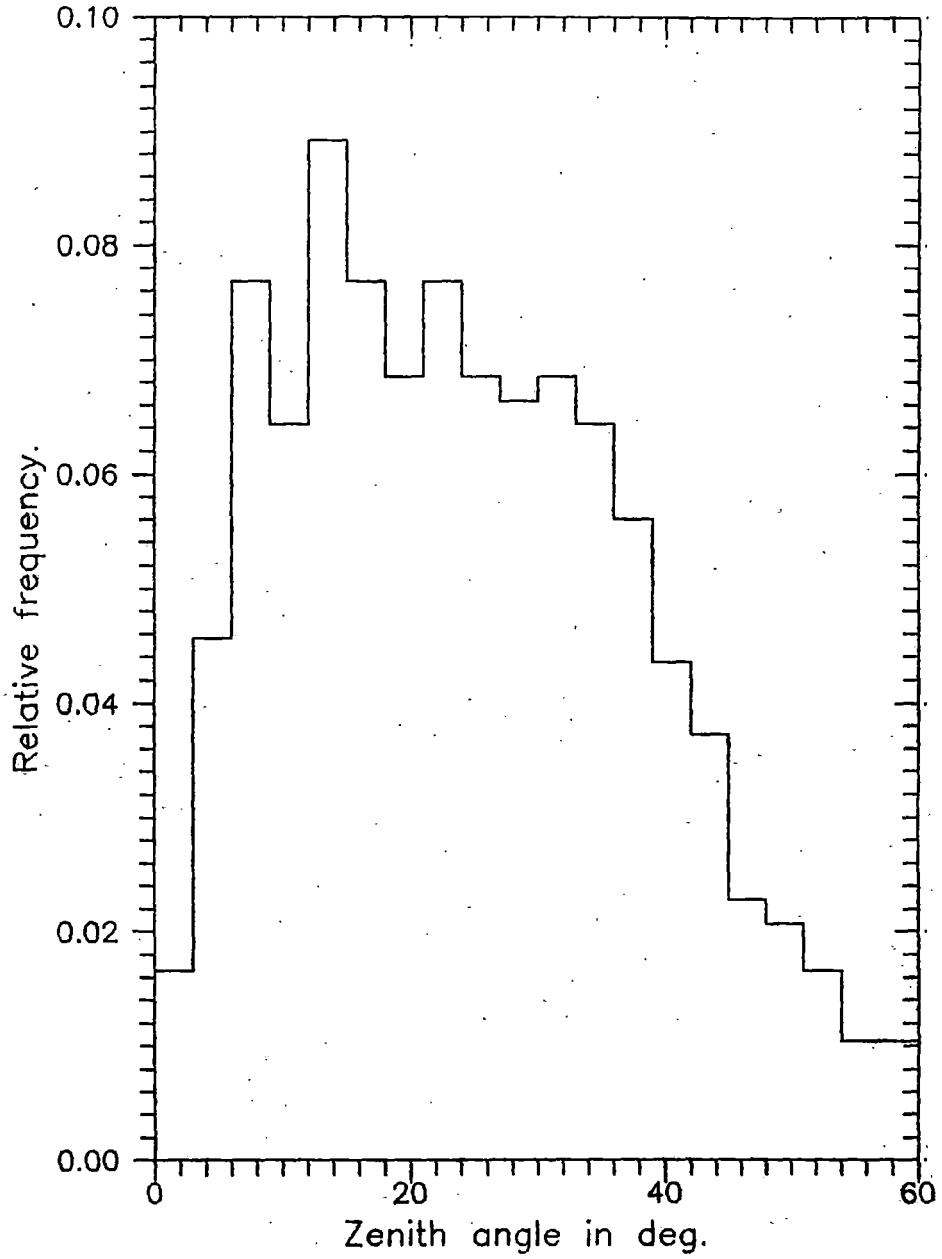

Fig.4.1h.
Zenith angle distribution of the observed showers in the shower size range $(4-9)X10^4$.

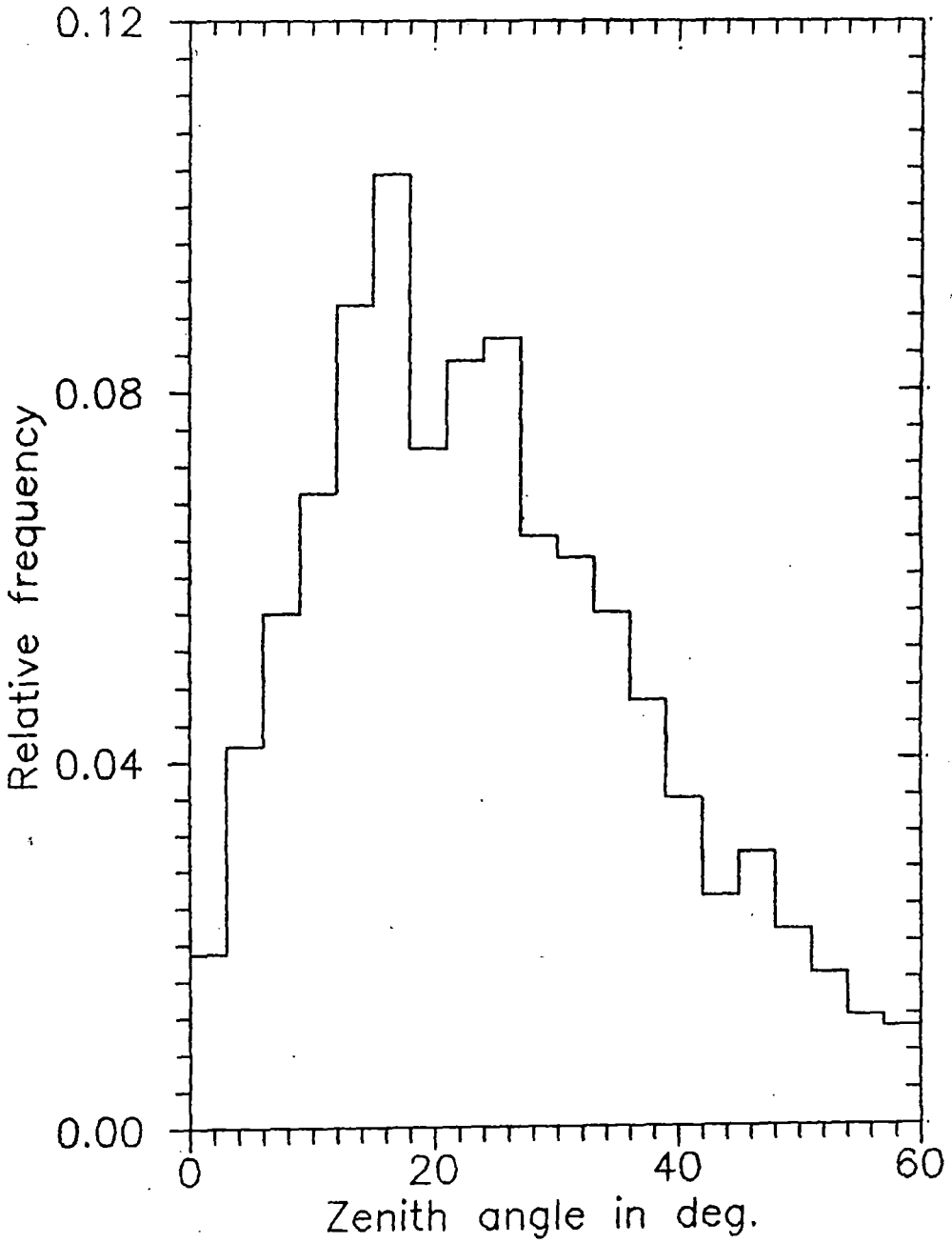

Fig.4.1i.
Zenith angle distribution of the observed showers in the shower size range $9X10^4-2X10^5$.

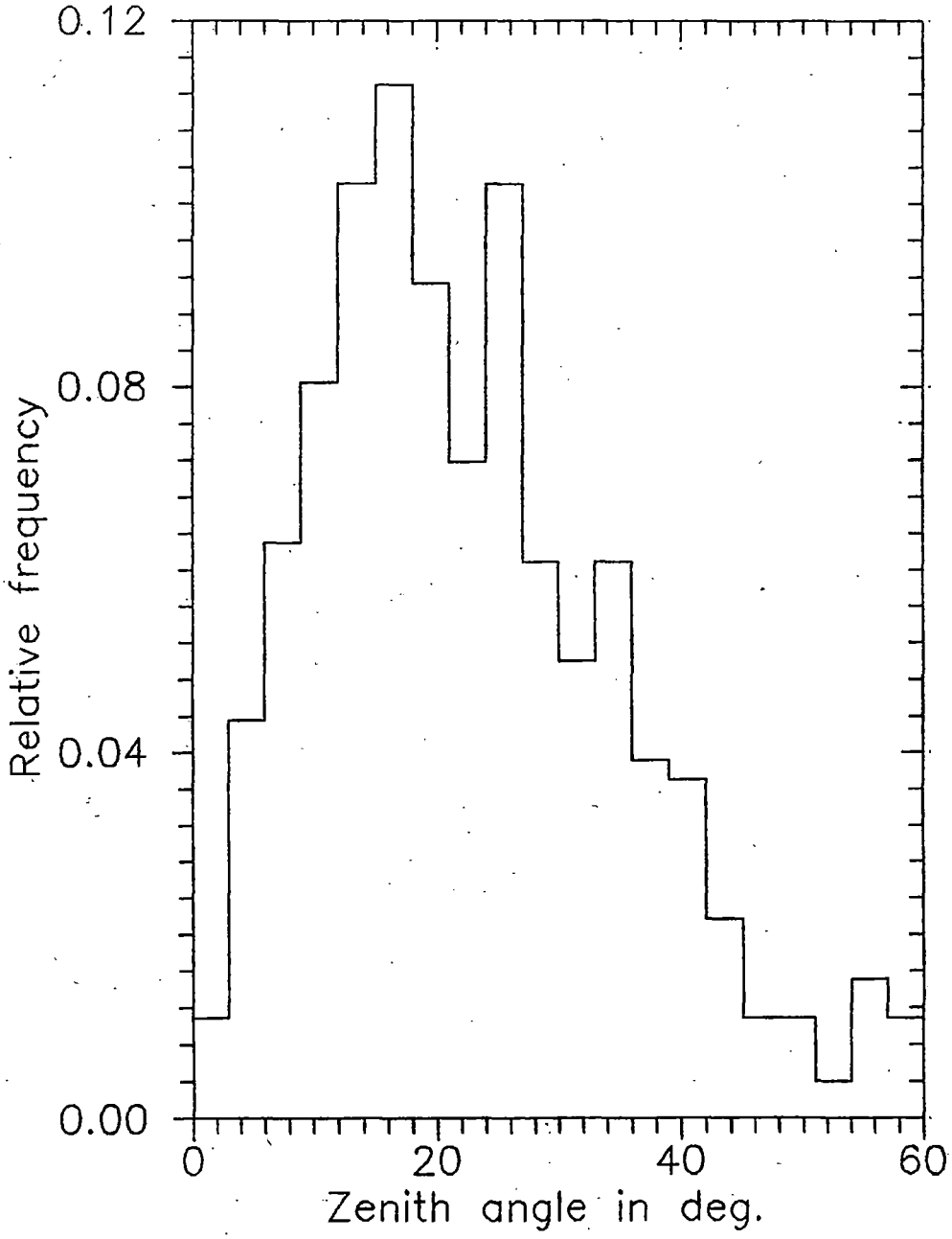

Fig.4.1j.
Zenith angle distribution of the observed showers in the shower size range $(2-5)X10^5$.

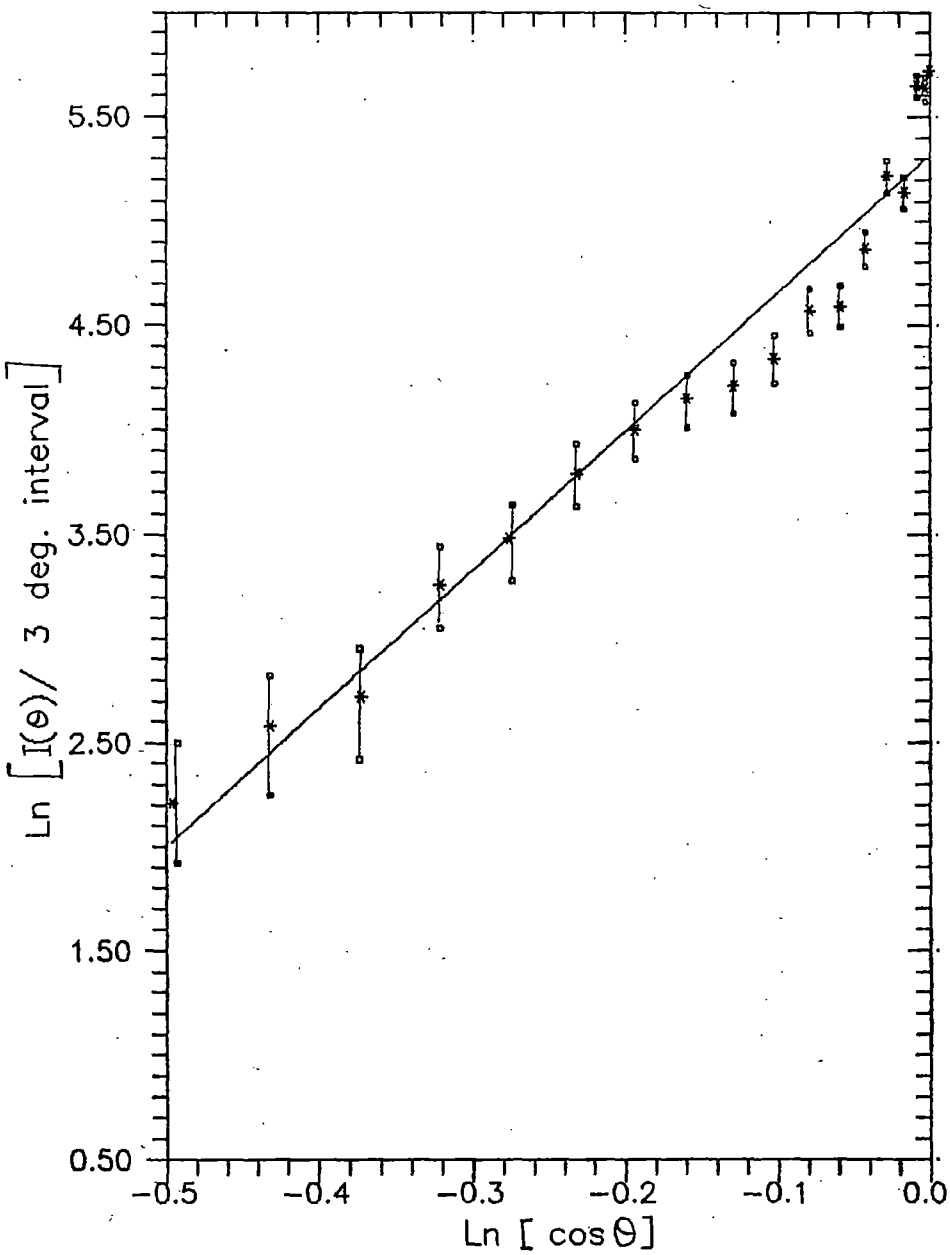

Fig.4.1k.
Variation of Ln(Intensity) vs. Ln(cosθ) for the shower size range $(4-9)X10^4$ particles.

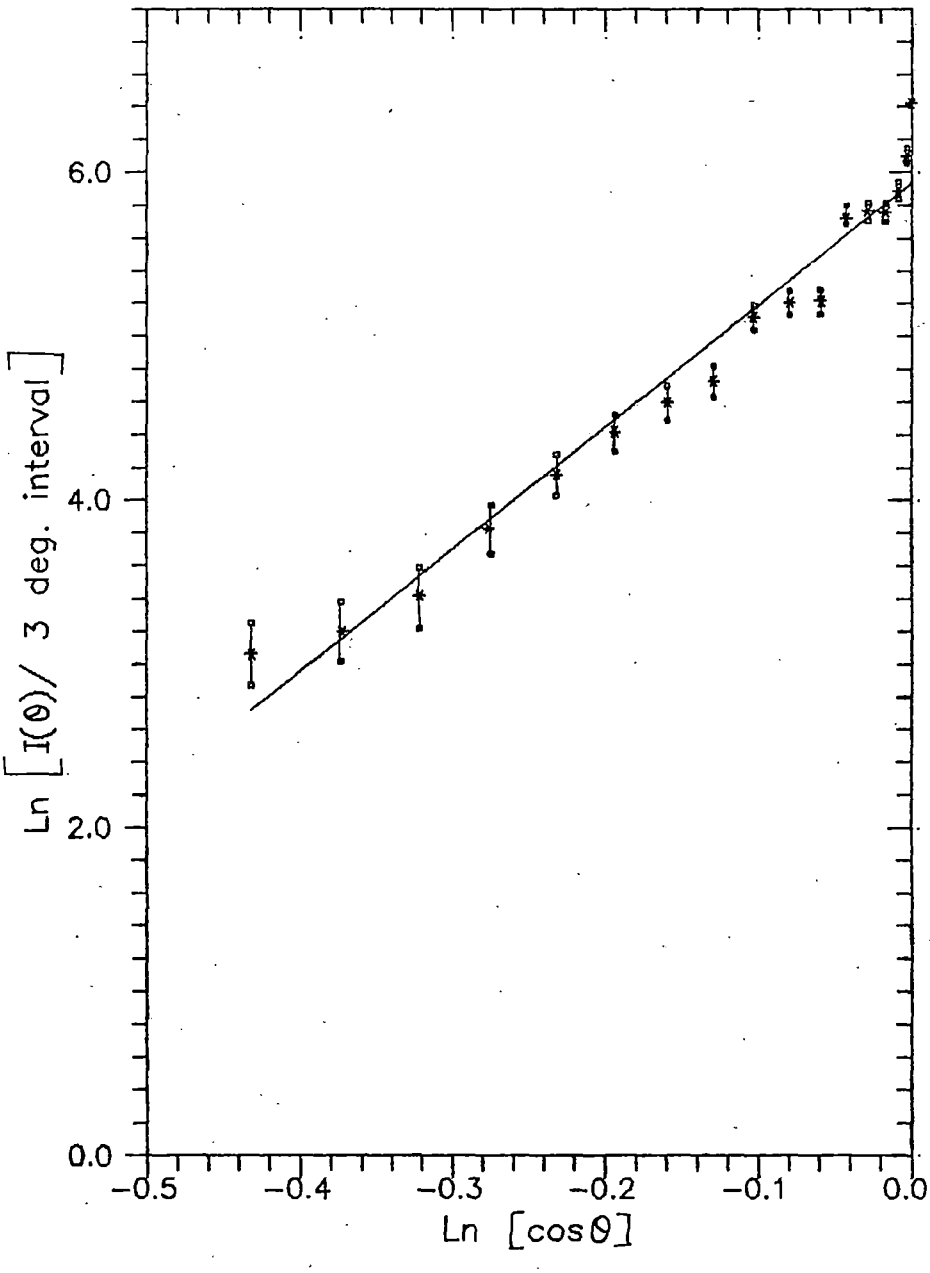

Fig.4.11.
Variation of Ln(Intensity) vs. Ln(cos θ) for the shower size range $9X10^4-2X10^5$ particles.

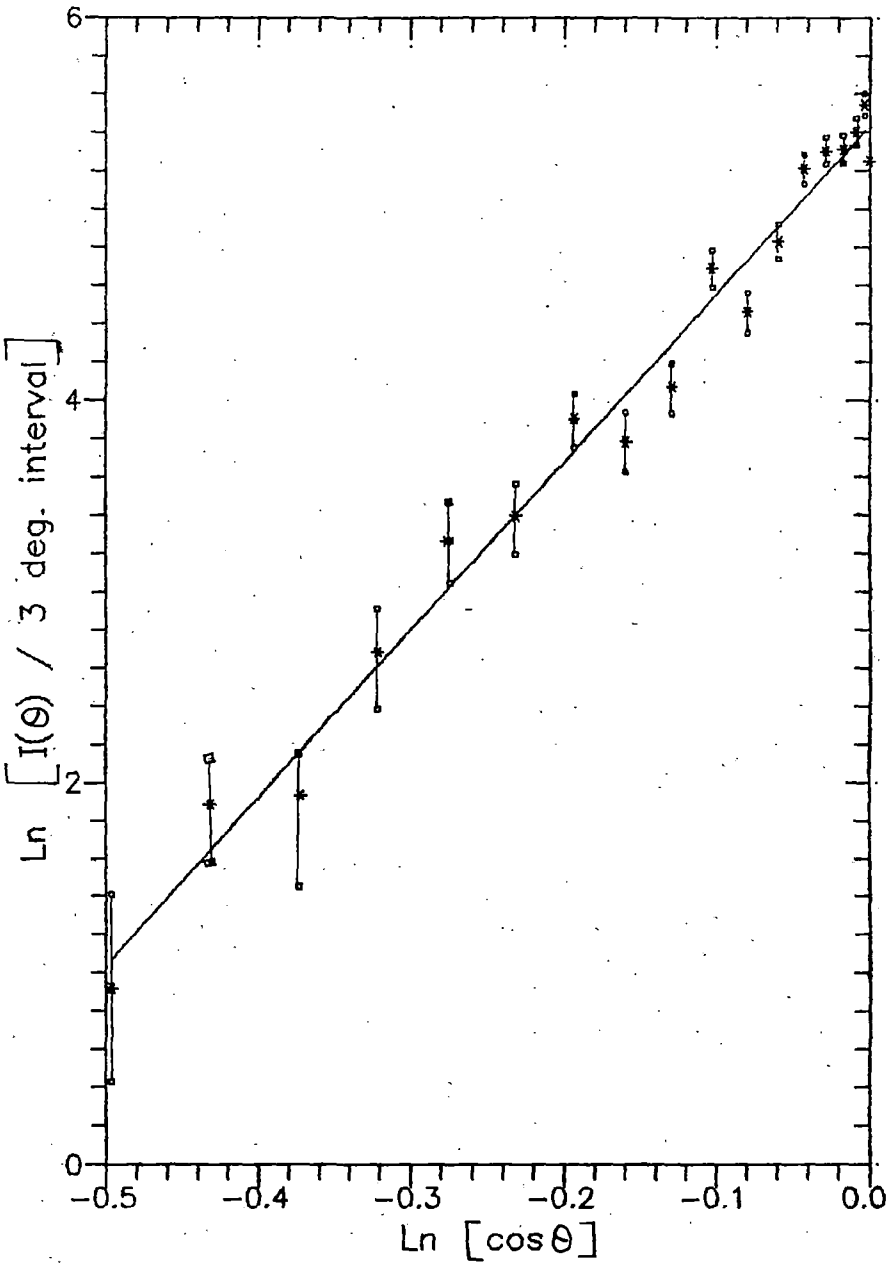

Fig.4.1m.
Variation of Ln(Intensity) vs. Ln(cosθ) for the shower size range $(2-5)X10^5$ particles.

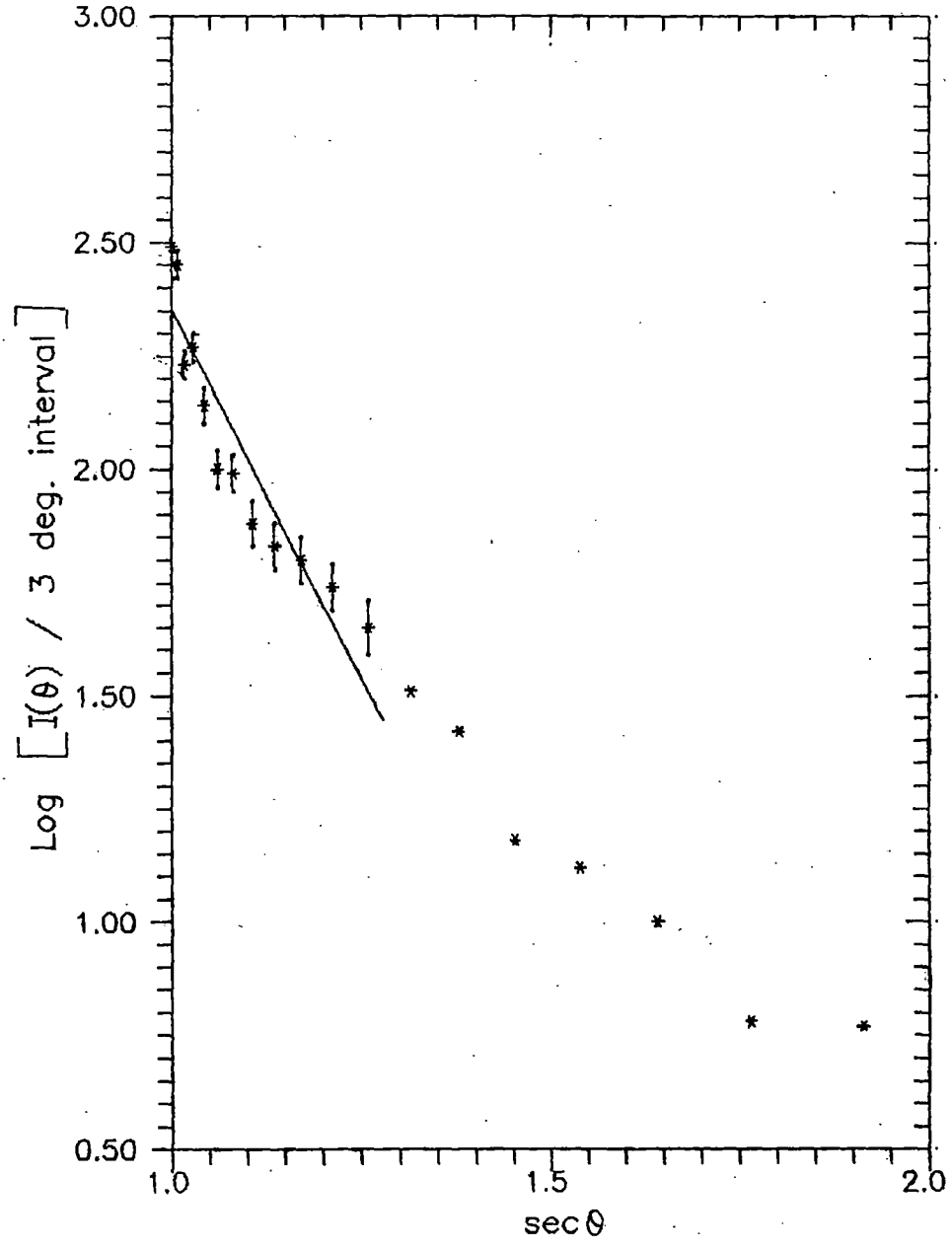

Fig.4.1n.
Variation of Log(Intensity) vs.secθ for the shower size range $(4-9)X10^4$ particles.

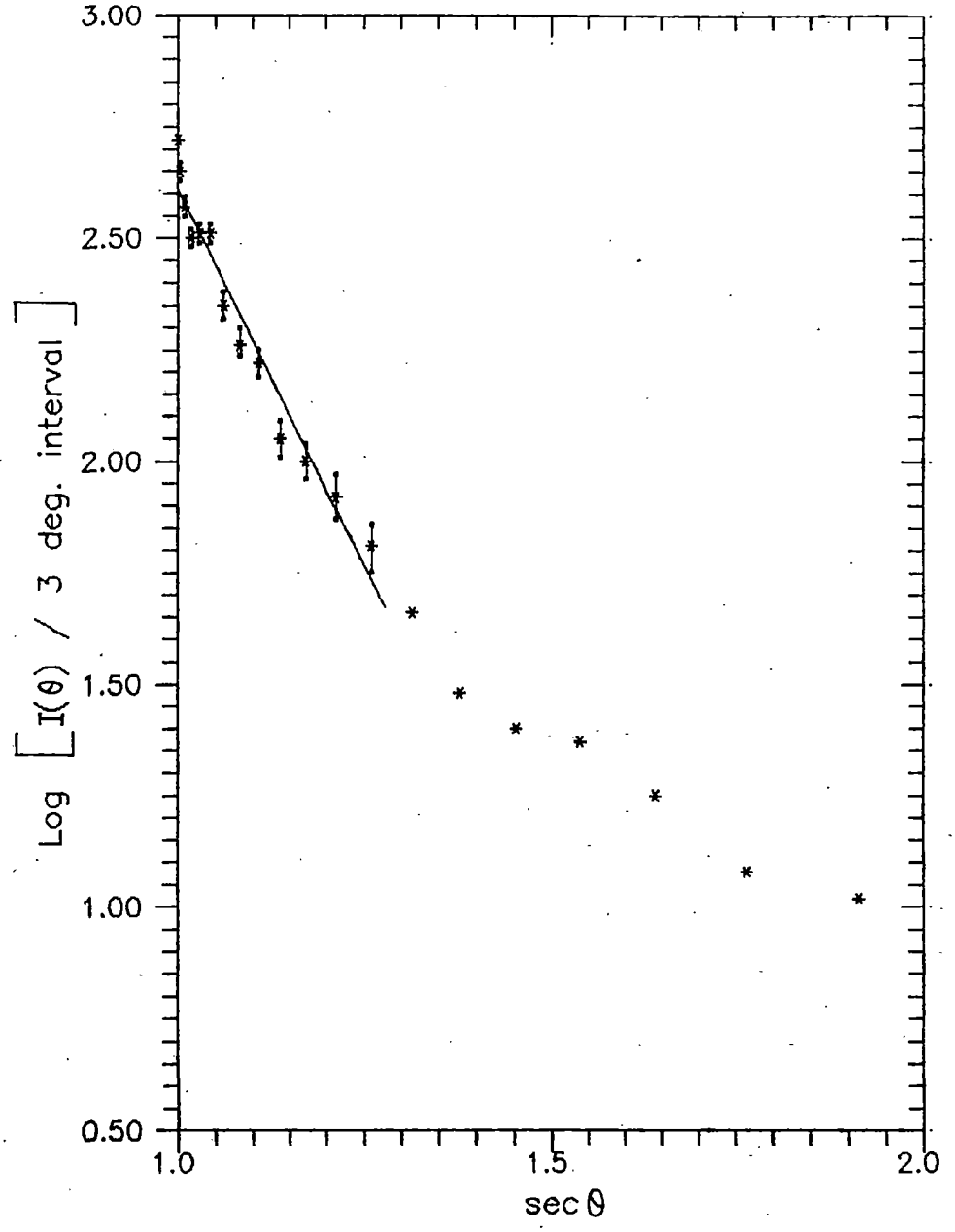

Fig.4.1o.
Variation of Log(Intensity) vs.secθ for the shower size range $9X10^4-2X10^5$ particles.

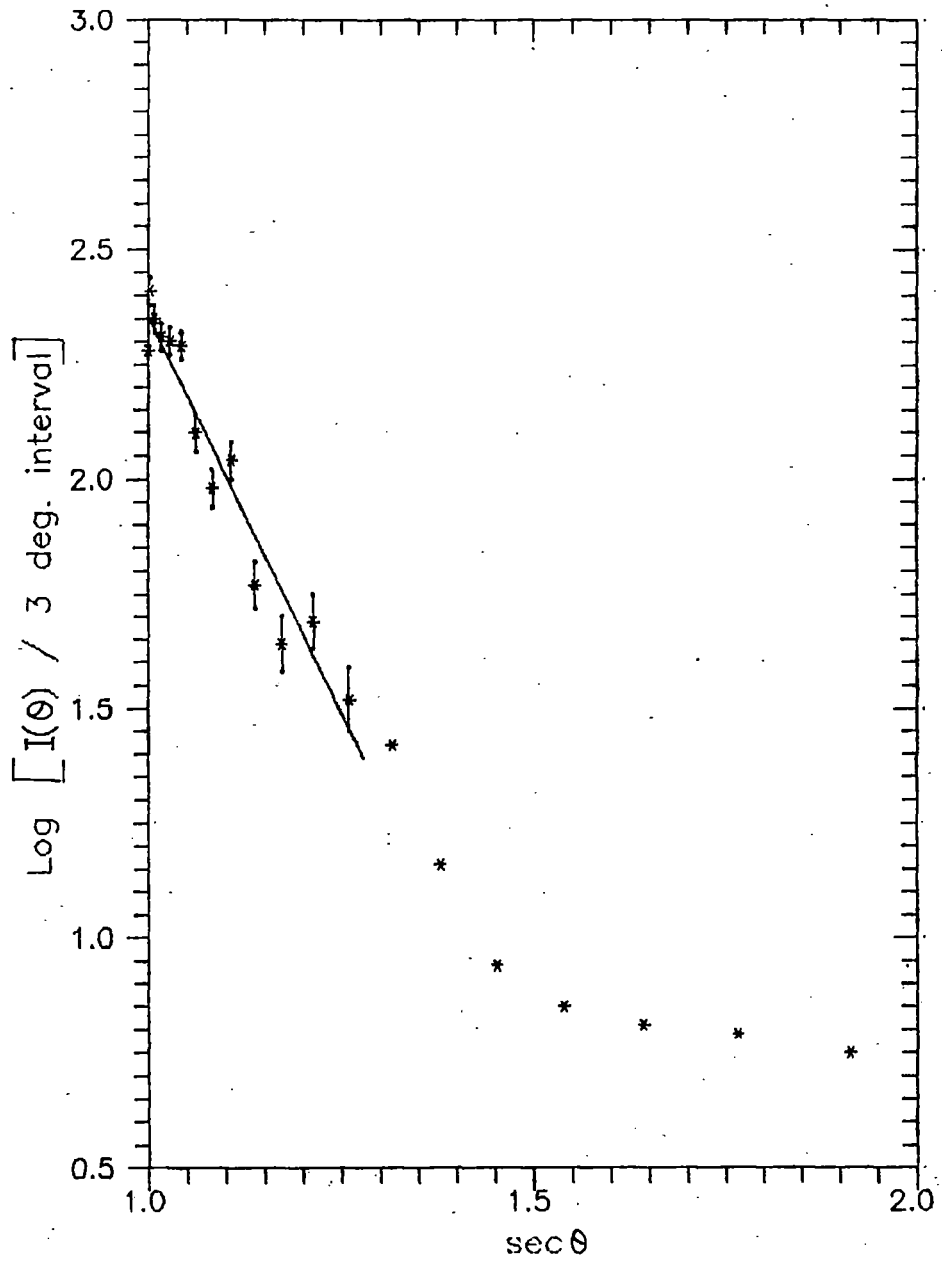

Fig.4.1p.
Variation of Log(intensity) vs. secθ for the shower size range $(2-5)X10^5$ particles.

values of the slope obtained by the Buckland Park array (Ciampa D. et. el. [4]) are bounded from -3.6 to -4.7.

Barometric coefficient from zenith angle distribution :

The variation of the rate of showers of a given shower size with change of barometric pressure is known as barometric coefficient. It can be shown that the barometric coefficient, B, written as dlnR/dp [=dlnR/dt] , where R is the shower rate , p is the atmospheric pressure and t is the atmospheric thickness in terms of atmospheric pressure , can be expressed by exponent of the zenith angle distribution and depth of observation.

The differential density spectrum i,e, the number of showers whose densities lie within the range Δ and $\Delta+d\Delta$ is found by experiment to be of the form (Galbraith W.[5])

$$\nu(\Delta)d\Delta = K.\Delta^{-\gamma-1}.d\Delta \quad \ldots\ldots\ldots \quad (4.1)$$

where γ is the power index of the spectrum.
and the differential shower size spectrum is

$$F(>N)\, dN = A.N^{-\gamma-1}.dN \quad \ldots\ldots\ldots\ldots(4.2)$$

where A is a constant.

Taking the average number of shower particles , $N(t,E_o)$ at a vertical depth t in the atmosphere arising from a primary of energy E_o as

$$N(t,Eo) = B.E_o^{\delta} \quad \ldots\ldots\ldots\ldots(4.3)$$

where B is a constant and δ is a slowly varying function of E_o,
We have took the integral energy spectrum of primary particles as (Galbraith W.[6])

$$I(>E_0) = K_2.E_0^{-\gamma'} \quad \text{.....(4.4)}$$

where $\gamma' = \delta\gamma$.

Let us consider a shower axis incident at a zenith angle θ to the vertical at a vertical depth t. Then number of particles at a depth of t' (t.secθ) beyond the maximum , produced by a primary particle of energy E_0 is taken to be of the form-

$$N(t',E) = K_1 E_0^{\delta} e^{-\lambda t'} \quad \text{.....(4.5)}$$

where λ is attenuation coefficient of the showers.

Therefore,

$$R(>N)_\theta = K_2.(N.e^{\lambda t}/K_1)^{-\gamma'/\delta} = K_3.N^{-\gamma}.e^{-\gamma\lambda t'} \quad \text{.....(4.6)}$$

$$dR = K_3.N^{-\gamma}.(-\gamma\lambda).e^{-\gamma\lambda t'}.dt'$$

$$dR/R = (-\gamma\lambda)\, dt' = d(\ln R) \quad \text{.....(4.7)}$$

Therefore,

$$-d(\ln R)/dt' = \gamma\lambda = 1/\Lambda \quad \text{.....(4.8)}$$ [Λ = absorption length] of the showers.

From (4.6), $R(>N)_\theta = K_3.N^{-\gamma}.e^{-\gamma\lambda.t\sec\theta}$

Considering θ small, $\sec\theta \sim 1+\theta^2/2$

$$R(>N)_\theta = K_3.N^{-\gamma}.e^{-\gamma\lambda t.(1+\theta^2/2)}$$
$$= K_3.N^{-\gamma}.e^{-\gamma\lambda t}.e^{-\gamma\lambda t\theta^2/2}$$

$$R(>N)_\theta = R(>N)_0.e^{-\theta^2/2\sigma} \quad \text{.....(4.9)}$$

where $R(>N)_0 = K_3.N^{-\gamma}.e^{-\gamma\lambda t}$ and $\sigma^2 = 1/\gamma\lambda t = \Lambda/t$.

Thus zenith angle distribution is a Gaussian with standard deviation σ.

Again from cosine power form of the zenith angle distribution (section 1.2.4., chapter-1) we can write,

$$R(>N)_\theta = R(>N)_o.\cos^n\theta$$

Expressing $\cos^n\theta \sim (1-\theta^2/2)^n = 1-n\theta^2/2 = e^{-n\theta^2/2}$

$$R(>N)_\theta = R(>N)_o.e^{-n\theta^2/2} \quad \text{.....(4.10)}$$

Therefore comparing equns. (4.9) & (4.10) we get,

$$n = t/\Lambda. \quad \text{.....(4.11)}$$

$\therefore$ Barometric coefficient, $B \sim 1/\Lambda = (n/t).100\%$
At sea level, t = 76 cm. of Hg.

$$B = 1.32.n\ \%\ \text{cm.}^{-1}\text{Hg.} \quad \text{.....(4.12)}$$

From this relation, barometric coefficient for the three shower size ranges (4-9)X10^4, (9X10^4-2X10^5), (2-5)X10^5 has been measured and shown in table-2. Measured values of barometric coefficient by Farley (Galbraith W.[7]) and Hodson (Hodson L. [8])for different shower size are also shown in table-2.

Table-2

Present Experiment	N_e	6.5 X10^4	1.45 X10^5	3.5 X10^5
	B (cm.$^{-1}$Hg)	8.76 %	9.83 %	11.58 %
Farley	N_e	1X10^4	3X10^4	3X10^5
	B(cm.$^{-1}$Hg)	10.2 %	11.1%	13.9 %
Hodson	N_e	5X104		
	B (cm.$^{-1}$Hg)	9.3%		

Table-2 : Barometric coefficient for different shower sizes.

Thus measured barometric coefficient increases with the increase of shower size. This result is consistent with the result of Farley, but discrepancy in the values are expected to be due to the fact that the exponents (n) of the zenith angle distribution are obtained from observations up to zenith angle 60^o.

Inference:

The measured barometric coefficient ($\sim\gamma\lambda$) [equation 4.8] increases with the increase of shower size. Assuming attenuation coefficient (λ) is constant, the measured barometric coefficient increases, this indicates that, with the increase of primary energy, primary spectrum index (γ) increases.

Absorption length of EAS from zenith angle distribution:

The absorption length (Λ) of EAS in the atmosphere can be obtained from zenith angle distribution.
From equation (v), the absorption length of EAS is of the form-

$$\Lambda = t/n$$

where t is the sea level atmospheric depth = $\sim$1000gm./cm^2 and n is the power index of zenith angle distribution obtained from the fig.4.1k, 4.1l and 4.1m for different sizes.

Table-3

	N_e	$(4\text{-}9)\times10^4$	$9\times10^4\text{-}2\times10^5$	$(2\text{-}5)\times10^5$
Present Expt.	Λ (gm/cm^2)	150	134	114
	N_e	$(1\text{-}3)\times10^5$	$3\times10^5\text{-}10^6$	$>10^6$
Asakimori et al.	Λ (gm/cm^2)	120±7	109±12	115±15

Table-3 Absorption length for different shower sizes.

The absorption length for different shower sizes is shown in table-3 along with the result of Asakimori (Asakimori K.et al.[9]). The result is consistent with the result of Asakimori in the size range (1-5)X10^5 obtained by a different method within the experimental uncertainties.

Azimuthal angle distribution:

Since the ultra high energy primary cosmic rays are highly isotropic, the azimuth angle distribution of cosmic ray air showers is expected to be uniform. The azimuth angle distribution of the observed showers is given in fig.4.1q. The distribuiton is consistent with the expectation.

4.1.4 Shower size spectrum:

Since the discovery of EAS , measurement of precise size spectrum has been one of the subjects of interest because of its direct dependence on the energy spectrum of primary cosmic radiation. In order to measure size spectrum, showers are taken within the size range 8X10^4 - 1.2X10^6 particles with their cores falling within the array and zenith angle $\leq 35^o$. Here the integral intensity of the size spectrum of EAS was calculated by approximation-

$$I(\geq N_e) = \Sigma u_k \sim \Sigma v_k/P_k(N_e,s)$$

where u_k and v_k are the expected and registered intensity of EAS , $P_k(N_e,s)$ is the triggering probability as described in section 3.3.2 of chapter-3, and k is the interval number. Flux is calculated by dividing the intensity by effective area (sec.3.3.2, chapter-3) and total observation time of the observed EAS.

The integral size spectrum obtained in the above procedure is given in fig.4.1r. Clearly a " kink " i.e., 'sudden change of exponent of the spectrum of power law' is observed at the shower size (5-7)X10^5. And the value of the exponent changes from (1.41 ± 0.067) to (2.16 ± 0.19) before and after the ' knee' position. Thus the integral size spectrum of the observed EAS in the shower size range 8X10^4 - 1.2X10^6 particles can be represented by power law with the form-

$$I(>N_e) = (1.50 \pm 0.048) \text{ X } 10^{-6} \text{ X } (N_e/10^5)^{(-1.41 \pm 0.067)} /m^2.s.sr.$$

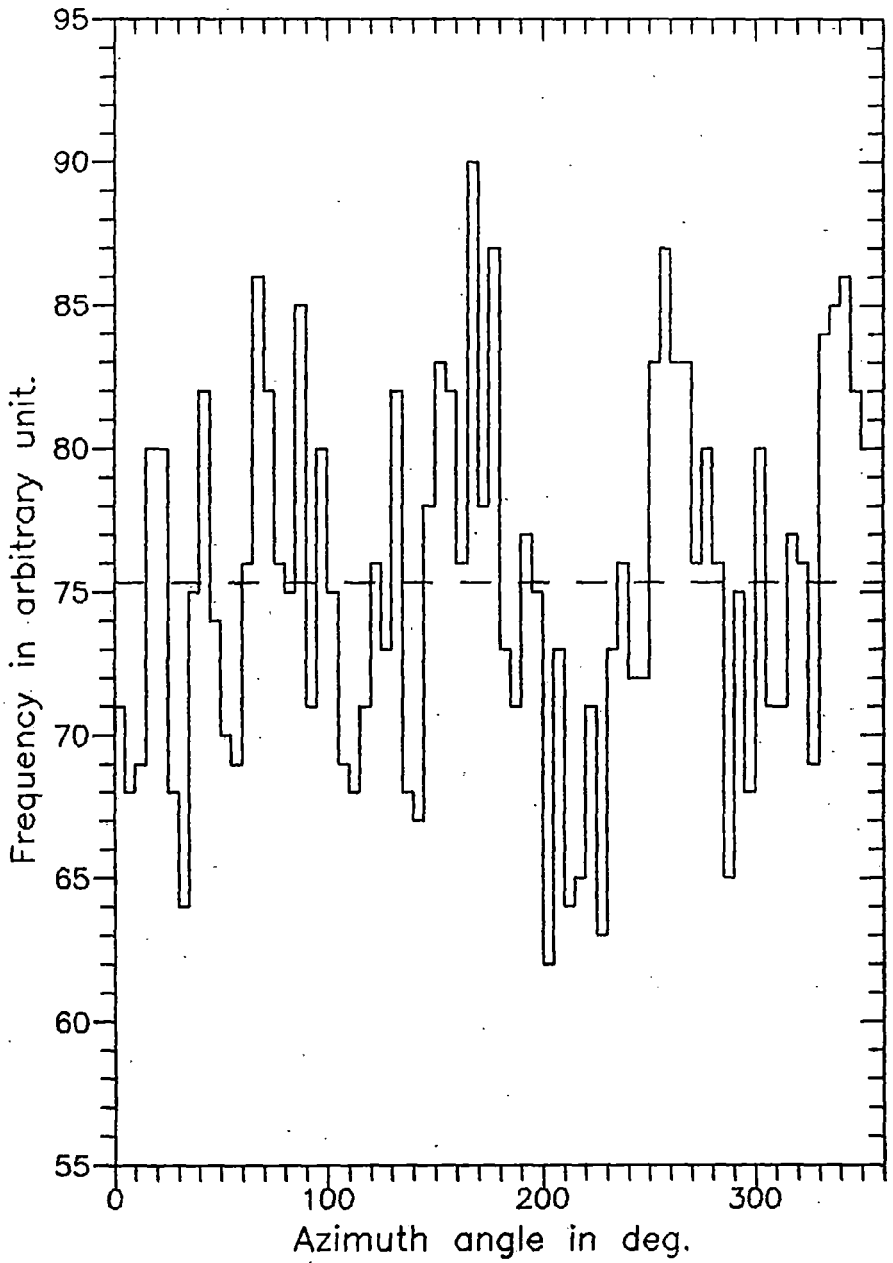

Fig.4.1q.
Azimuth angle distribution of the observed shower events.

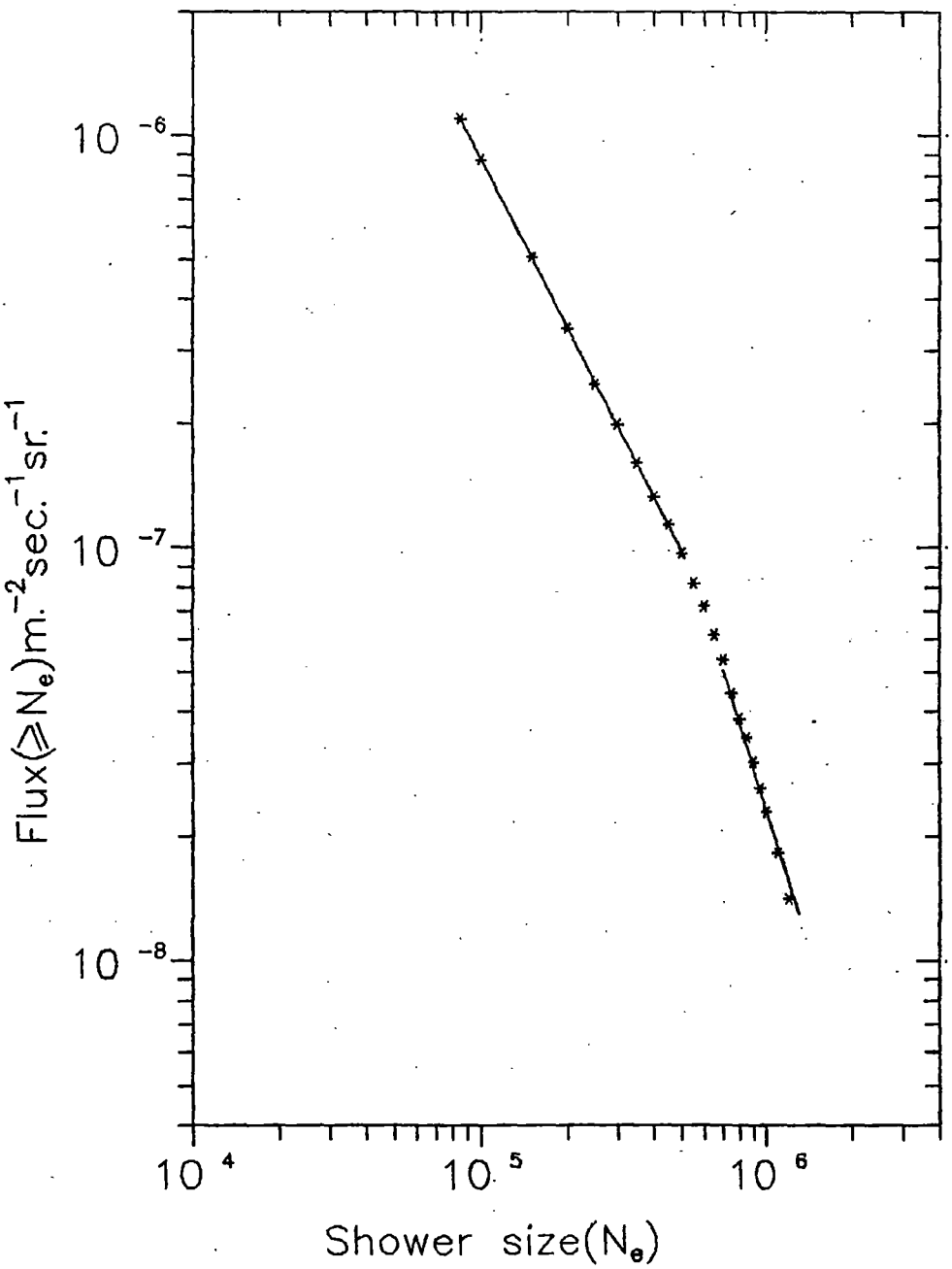

Fig.4.1r.
Integral shower size spectrum of the present experiment.

for $8 \times 10^4 < N_e < 5 \times 10^5$ and

$$I(>N_e) = (3.60 \pm 0.003) \times 10^{-6} \times (N_e/10^5)^{(-2.16 \pm 0.19)}/m^2.s.sr.$$

for $7 \times 10^5 < N_e < 1.2 \times 10^6$

Here difference between the two values of the power index (0.75) is slightly higher than the value (~0.5) reported previously. This is expected to be due to the two facts, (i) triggering probability is above 90% for $N_e > 2X10^5$ (see in fig.3.3f of chapter-3). Hence, here comes some error due to low triggering probability below this size. (ii) Again shower age below the size 10^5 particles is greater than the average value of the shower age for all showers. From the fig.3.3f of chapter-3 , it is clear that triggering probability is lower for larger shower age, as a result, some error comes in the spectral index measurement.

Table-4 shows the 'knee' of the shower size spectrum obtained by the different groups (Catz . Ph. et al[1], Atraskevitch. G.V. et al[10], Ashton. F. et al[11], Hara. T. et al[12], Aglietta M. et al[13], Danilova E.V. et al[14]) at various altitudes. The table shows that the position of the 'knee' changes about two times of the present result in between the sea level and in the mountain altitude.

Table-4 : Position of the 'knee' of integral shower size spectrum and 'knee' of the primary spectrum for different observation levels.

Table-4

Experiment	Observation level	'Knee' position (N_e)	'Knee' of the primary spectrum(eV)
Present experiment	Sea level	$(5\text{-}7)X10^5$	$(2.75\text{-}3.69)X10^{15}$
Catz, Ph. et al	Sea level	$10X10^5$	$5.03\ X10^{15}$
Atraskevitch G.V. et al	Sea level	$4\text{-}5X10^5$	$(2.27\text{-}2.75)X10^{15}$
Ashton F. et al	Sea level	$5\text{-}8X10^5$	$(2.75\text{-}4.14)X10^{15}$
Hara T. et al	900 m.a.s.l.	$8\text{-}10X10^5$	$(4.14\text{-}5.08)X10^{15}$

Aglietta M. et al	2000 m.a.s.l.	$11X10^5$	$5.46X10^{15}$
Danilova E.V. et al	3250 m.a.s.l.	$7\text{-}10X10^5$	$(3.69\text{-}5.03)X10^{15}$

The results on variation of shower age(s) with shower size(N_e) from the sea level EAS observations [Gerhardy P.R. et. al.[15], Asakimori et al.(Tonwar S.C.[16])] show that with the increase of shower size (N_e), the shower age (s) slowly decreases. Since a 'knee' exists in the primary cosmic ray energy spectrum, so the results on $N_e \sim s$ correlations and electron-photon cascade theory suggest that, for old showers ($s > 1$), the 'knee' in the shower size spectrum should be in the region of small shower size (N_e). However in the MAKET-ANI experiment (section 1.5, chapter-1), totally opposite behaviour was observed. This result is interesting because it is also unexplainable by the suggestions of idea of dominance of the heavier primaries around $E \sim 10^{15}$ eV. This result from MAKET-ANI experiment is also in contradiction with the experimental observation of Danilova (Danilova E.V. et. al.[14]).

As it is known, the electron size at the maximum of shower development is one of the best primary energy estimators, and hence the mean energy of the primary particle has been obtained with a maximum error of 10% (which includes fluctuation in EAS development and the error in shower size measurement) from the energy scale established on the basis of hybrid Monte Carlo model (Trzupek L.G. et. al. [17]) for EAS at sea level as

$$E_0 = 3.03 \text{ X } 10^{10} \text{ X } N_e^{0.87} \text{eV}$$

The 'knee' of the primary energy spectrun, using the above conversion formula,corresponding to the 'knee' of the shower size spectrum of the observed showers (along with the results of others) is also shown in table-4. From the table, it is seen that some of the 'knee' energies of the primary spectrum are consistent with the 'knee' region at $3X10^{15}$eV reported by Simon P.S. (Simon P.S. et. al.[18]) .

4.2 **Study on shower 'age' parameter :**

The longitudinal development of cosmic ray EAS is an essential feature that reflects the gross feature of particle interaction at high energies. The stage of development of an air shower is described by shower 'age' parameter (s). The showers that develop early in the atmosphere have on the average larger 'age' than the late developing showers of equal primary energy. Discriminating of gamma ray initiated showers from the large background of charged cosmic ray initiated showers based on shower age has been used in several observations (Samorski and Stamm[19], Protheroe et al[20]) on the assumption that for same shower size , photon initiated showers are older. But the Monte Carlo simulation results (Fenyves J.[3], Hillas A.M.[21]) show that in 'age', the gamma ray induced showers are not older than that of the normal showers, though in several observations it is found that the excess showers from the direction of discrete point sources are characterised by high 'age' value (Samorski and Stamm[19], Tonwar S.C.[22]).
The results of the present study on variation of shower 'age' on shower size and zenith angle are given in section 4.2.1. and 4.2.2.

4.2.1. **Variation of shower 'age' with shower size :**

Distribution of the shower 'age' parameter (s) determined by the fitting of observed shower data to the ldf of Hillas in the range $0.6 < s < 1.8$ for the shower size bins $6.3X10^4$ - $1X10^5$, $2.5X10^5$ - $4X10^5$, $4X10^5$ - $6.3X10^5$ and $6.3X10^5$ - $1X10^6$ is shown in fig.4.2a, 4.2b, 4.2c and 4.2d. From the distributions, it is observed that the spread of the distribution becomes narrower with the increase of shower size. Similar trend in the shower age distribution was obtained by the Kobe group (Asakimori K. et al.[23]) and also by the Akeno group (Nagano M. et al.[24]). The relative variance of 'age' parameter (σ_s/s) with shower size is shown in fig.4.2e.

The variation of average shower age($\bar{s}$) with the average shower size ($\bar{N}_e$) for the observed shower events along with the experimental results of Buckland Park array (Gerhardy et. al. [15]) and Kobe group (Tonwar S.C.[16]) is shown in fig.4.2f. All the results show, that the average age parameter ($\bar{s}$) decreases with the increase of shower size at sea level. Present experimental result shows that the variation is within 15% w.r.t. the mean value, but in the case of Buckland Park and Kobe group, this variation is ~21%. Thus present experimental variation of shower age is less than the others. Error bars on few points are also shown in the figure.

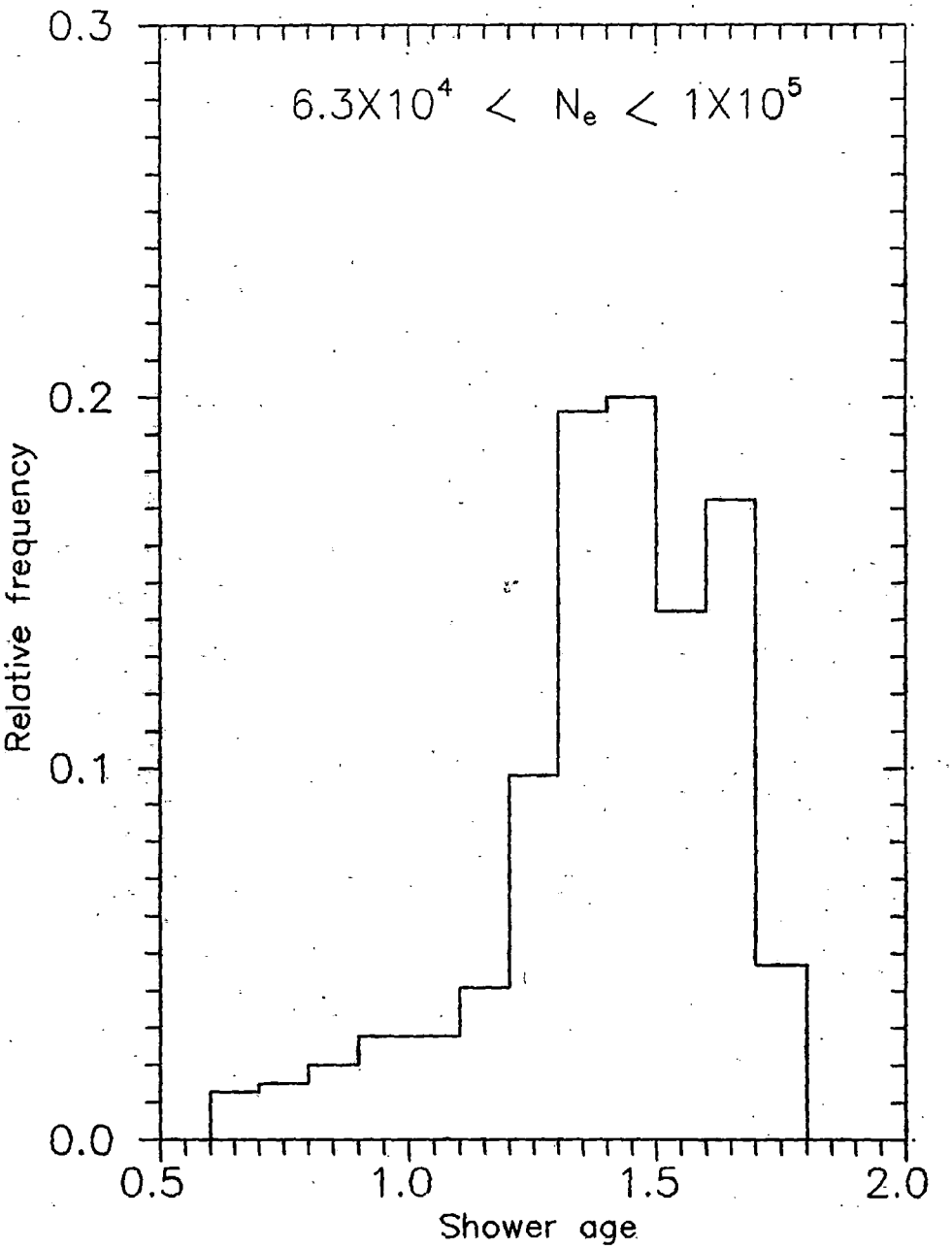

Fig.4.2a.
Shower age distribution for the shower size range 6.3 X 10^4 – $1X10^5$ particles.

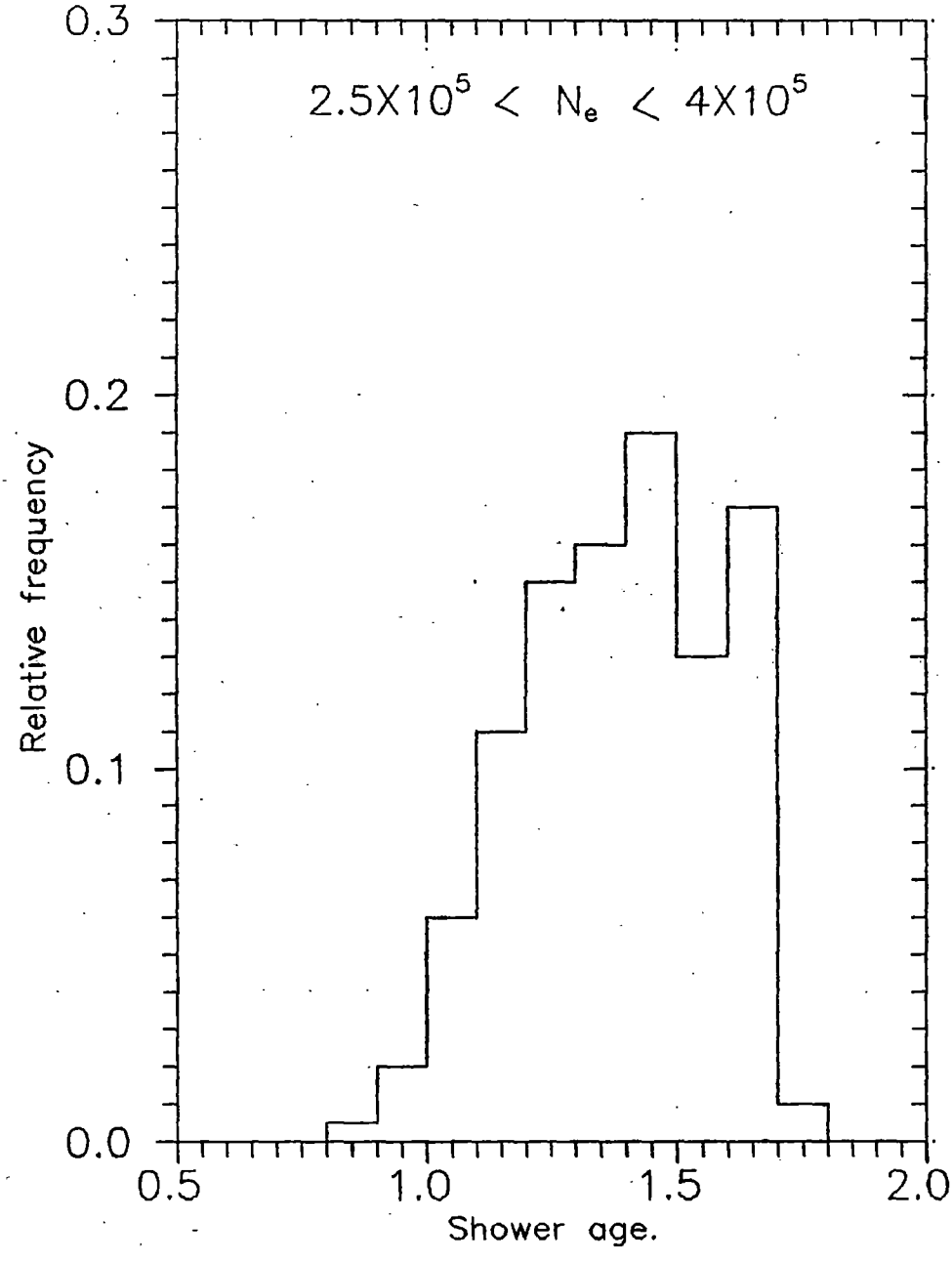

Fig.4.2b.
Shower age distribution for the shower size range $2.5X10^5 - 4X10^5$ particles.

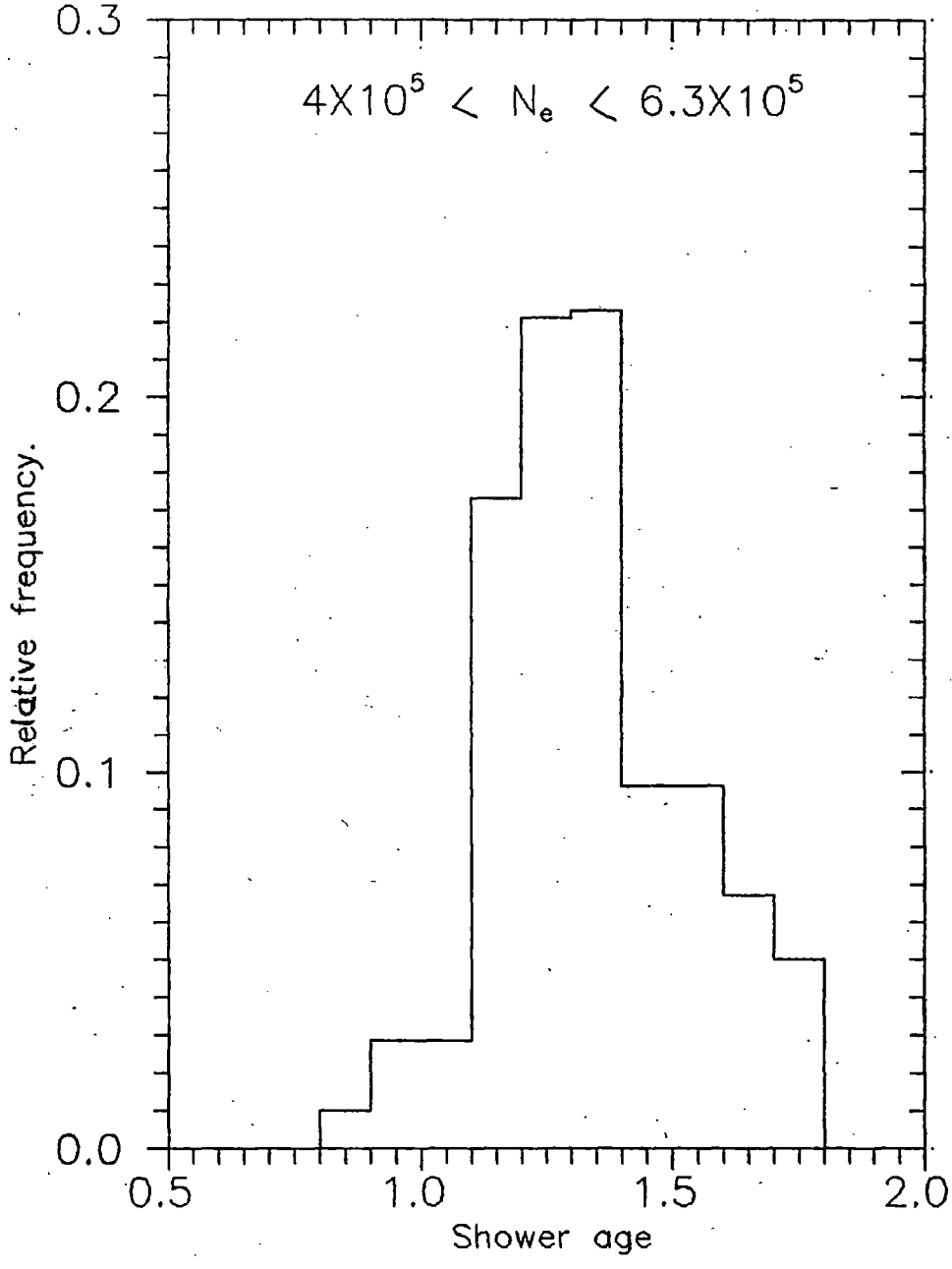

Fig.4.2c
Shower age distribution for the shower size range $4X10^5$ - $6.3X10^5$ particles.

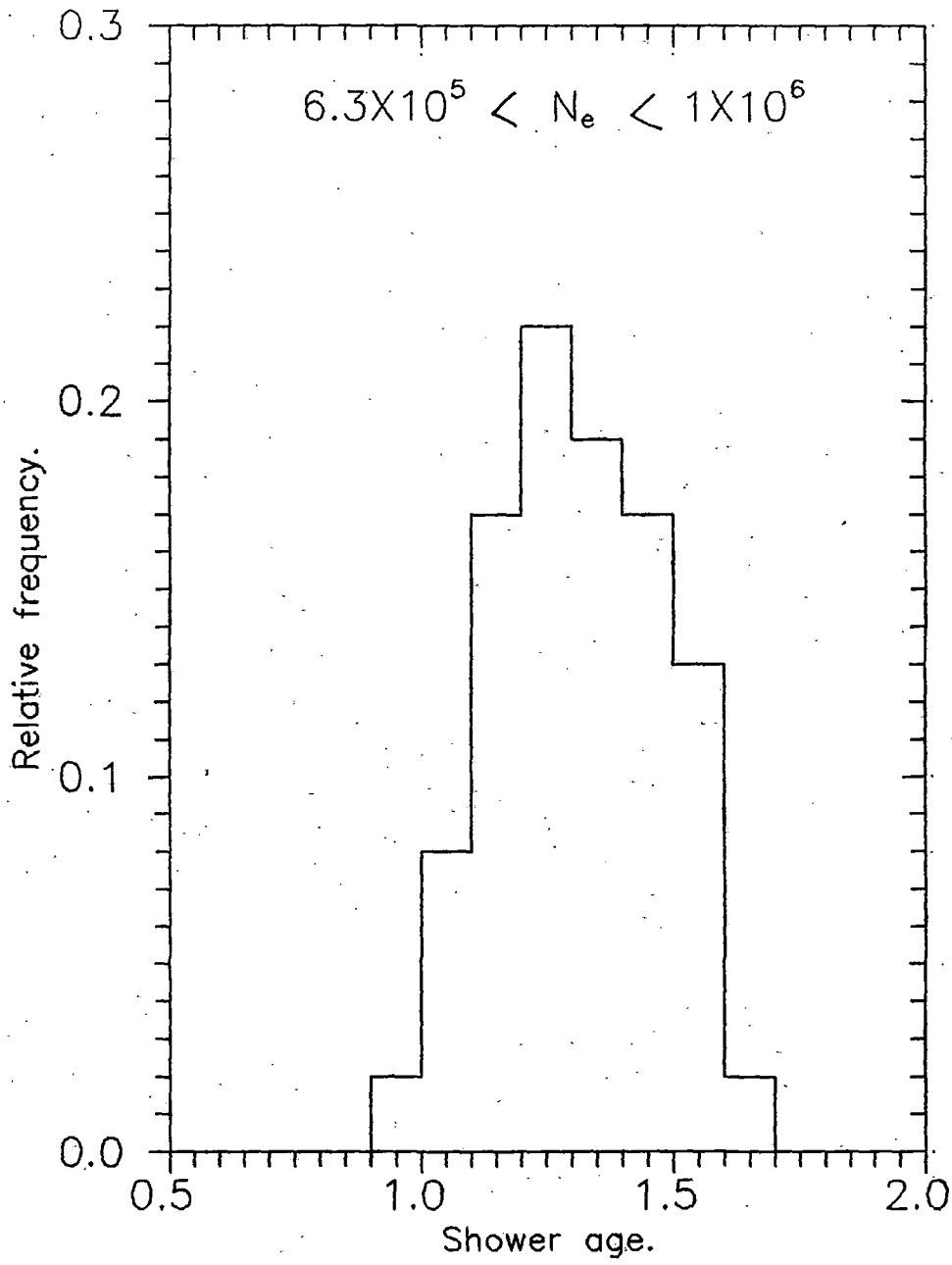

Fig.4.2d.
Shower age distribution for the shower size range $6.3X10^5$ – $1X10^6$ particles.

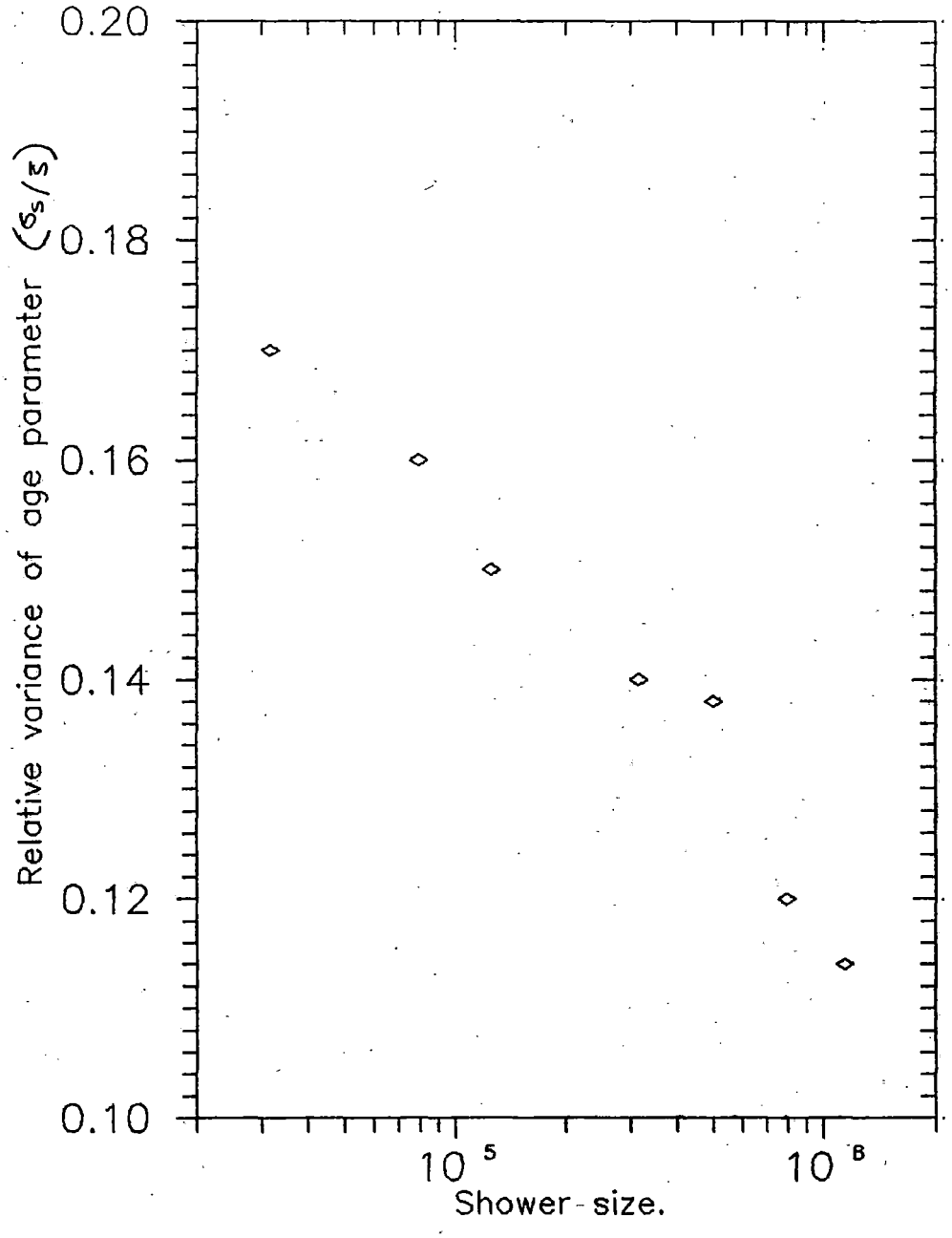

Fig.4.2e.
Relative variance of shower age with shower size.

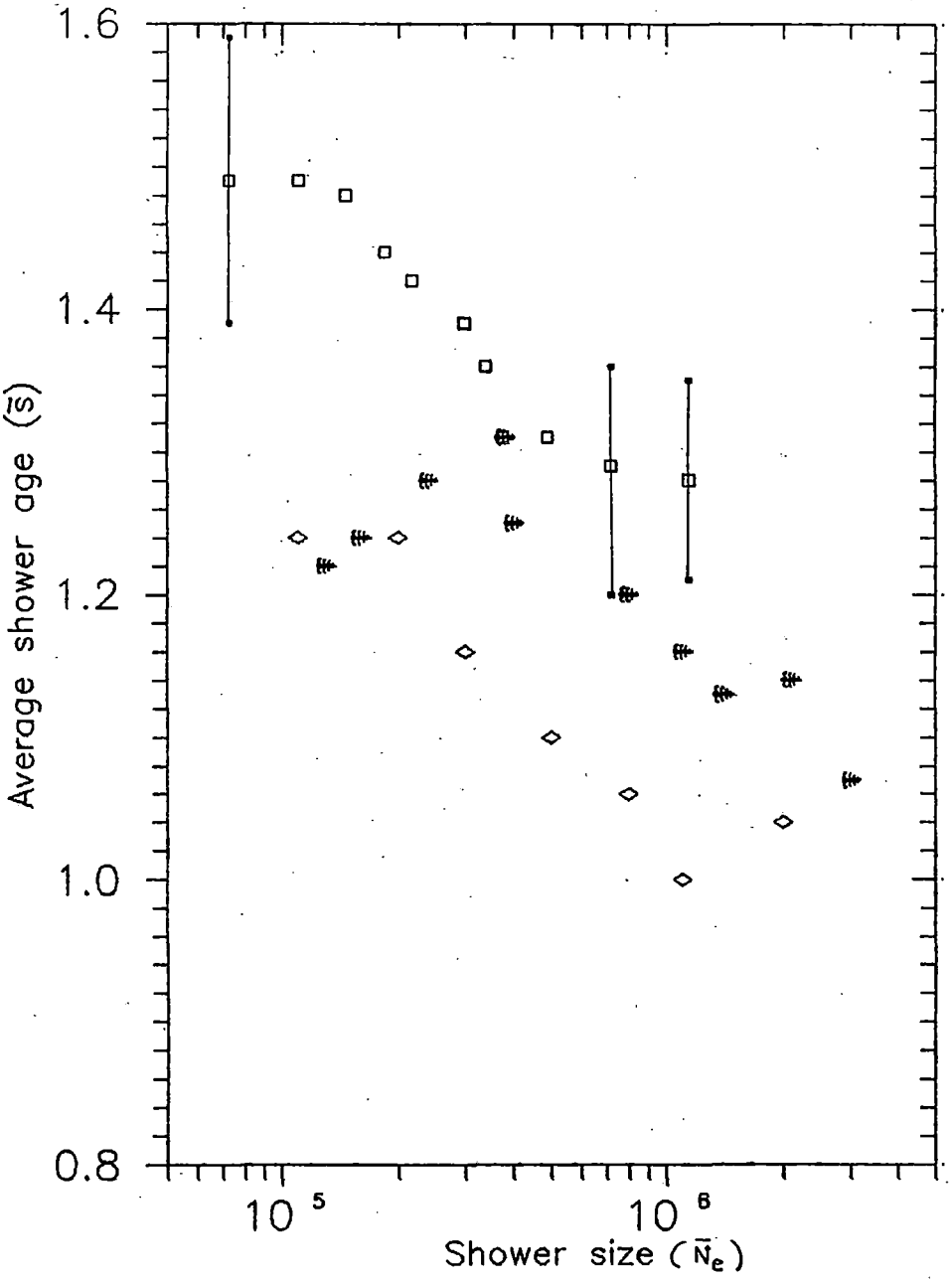

Fig.4.2f.
Variation of average shower age with shower size.
□ ..... Present experiment.
tt ..... Gerhardy et.al.
◇ ..... Asakimori et. al.

4.2.2. **Zenith angle dependence on shower 'age' :**

In some of the recent EAS observations, the showers from point sources were observed at large angles during most of the observation time due to high angle of transit of the sources at the arrays. For example, Cygnus X-3 is observed at Kiel at zenith angle about 14^o, the same source is observed at Ooty at zenith angle nearly 26^o at the transit. Though in the search for evidence for UHE emission the source and the background events are collected during the same time in the same zenith angle intervals still there is a remote possibility (because of small statistics) that the source events had higher zenith angle than the background events. And with the increase of zenith angle , the atmospheric thickness increases, so showers with high zenith angles are expected to have high shower 'age' value. To understand the problem, dependence of shower 'age' on zenith angle in the range 0^o - 55^o is examined.

The variation of mean shower 'age' ($\bar{s}$) with zenith angle is shown in fig.4.2g. The variation of $\bar{s}$ with zenith angle (θ) is found slow and up to zenith angle 30^o the shower 'age' is practically found to be independent of zenith angle. The variation of mean shower age with zenith angle for three shower size ranges, $(5\text{-}8)X10^4$, $(9X10^4\text{-}1.5X10^5)$, $(1.5X10^5\text{-}5X10^5)$ are shown in fig.4.2h, 4.2i and 4.2j. The observed variation can be expressed by the relation

$$s = A .\sec\theta + s_o$$

where the values of s_o and A for different shower size range are given in table-5.

The development of the electron - photon cascade is approximately described by the equations (Greisen K. [25])

$$s = 3t / (t + 2.W) \quad \ldots\ldots\ldots\ldots \quad (4.13)$$

$$\text{and } N_e = (0.31/ W^{0.5}). \exp [t(1 - 1.5. \ln(s))] \quad \ldots\ldots\ldots (4.14)$$

where $W = \ln.(E/\varepsilon_o)$ and t is the atmospheric depth in radiation length. Using equns. (4.13), (4.14) and expressing the variation of s with zenith angle for three

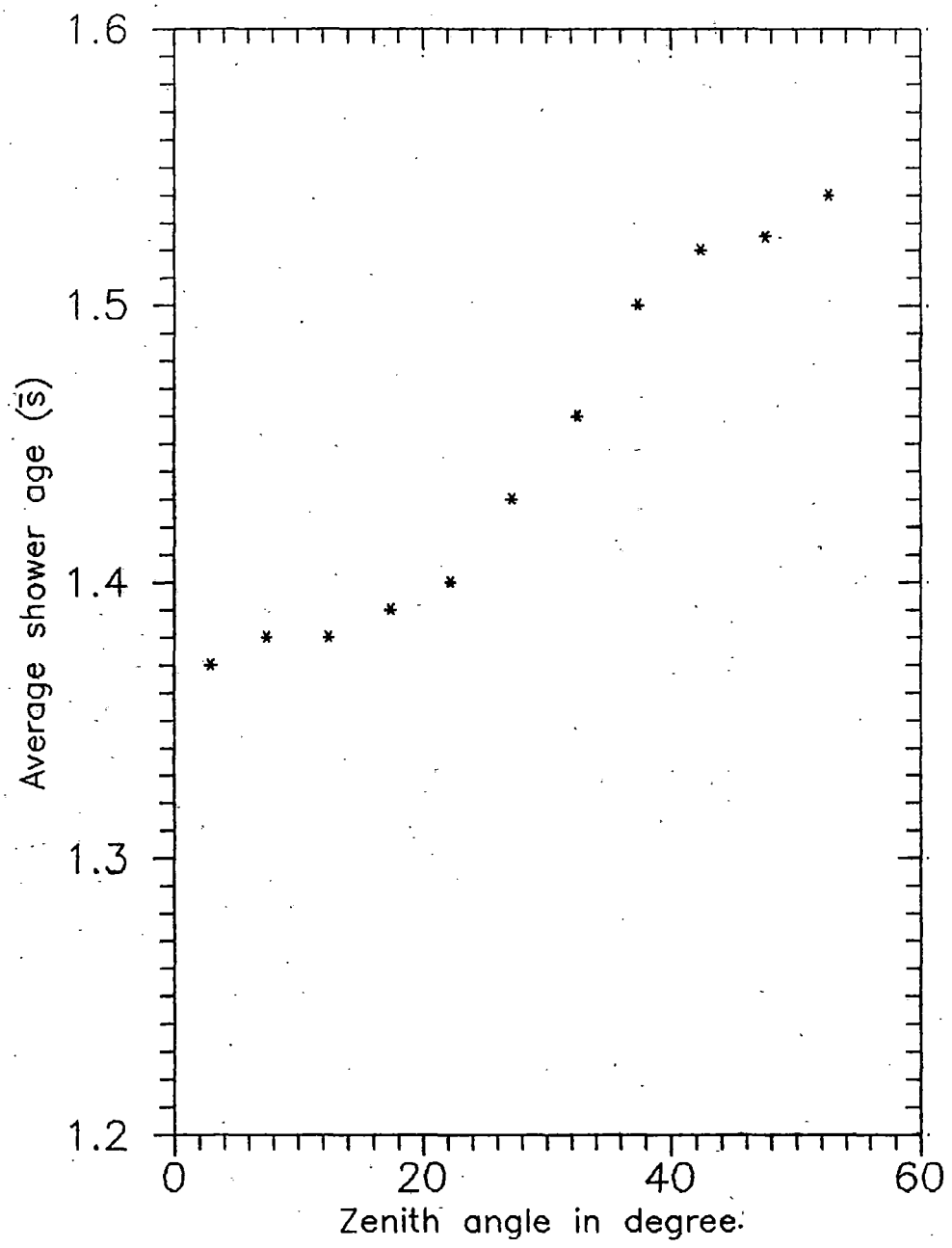

Fig.4.2g.
Variation of average shower age with zenith angle.

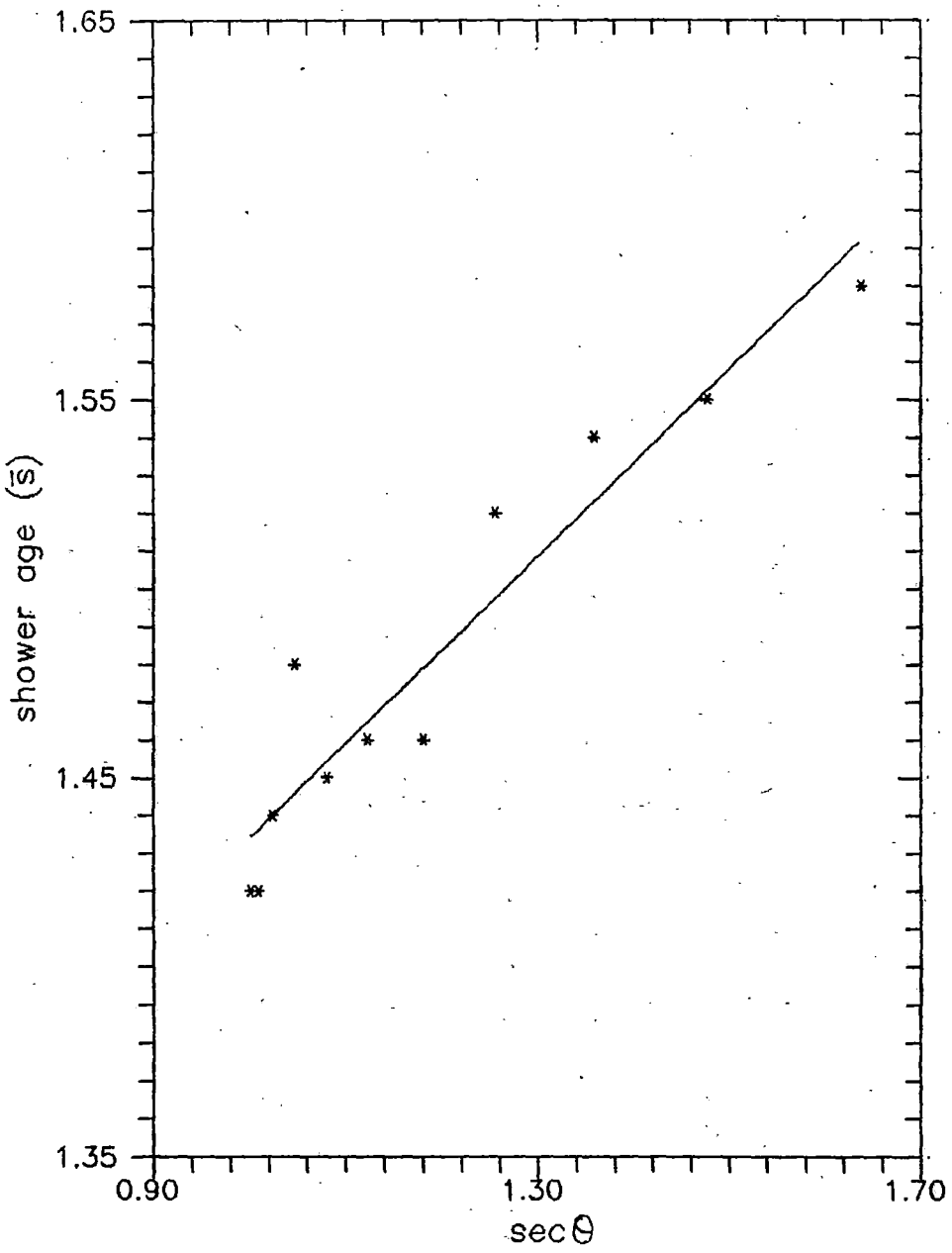

Fig.4.2h.
Variation of shower age with zenith angle for the shower size range $5X10^4-8X10^4$

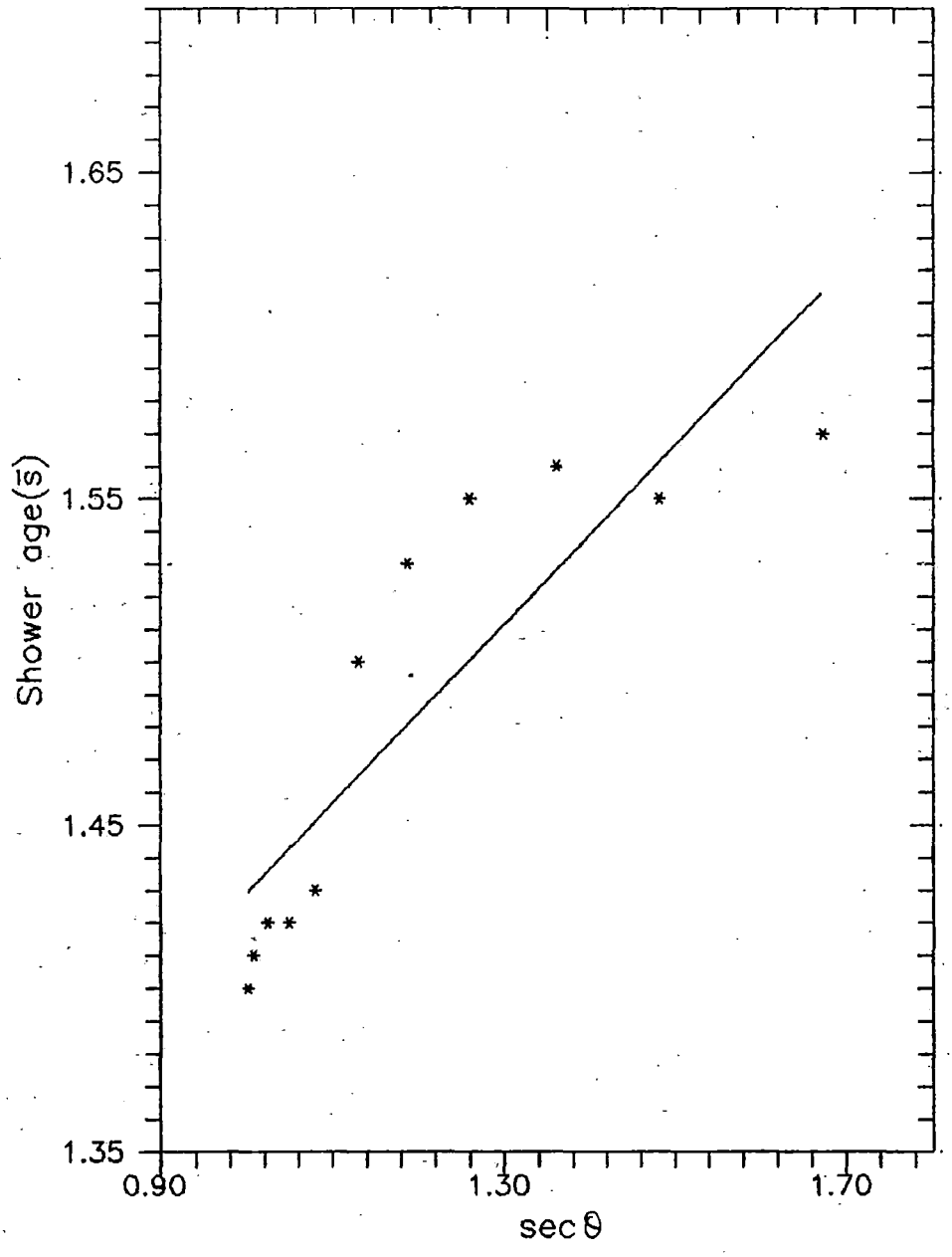

Fig.4.2i
Variation of shower age with zenith angle for the shower size range $9X10^4-1.5X10^5$

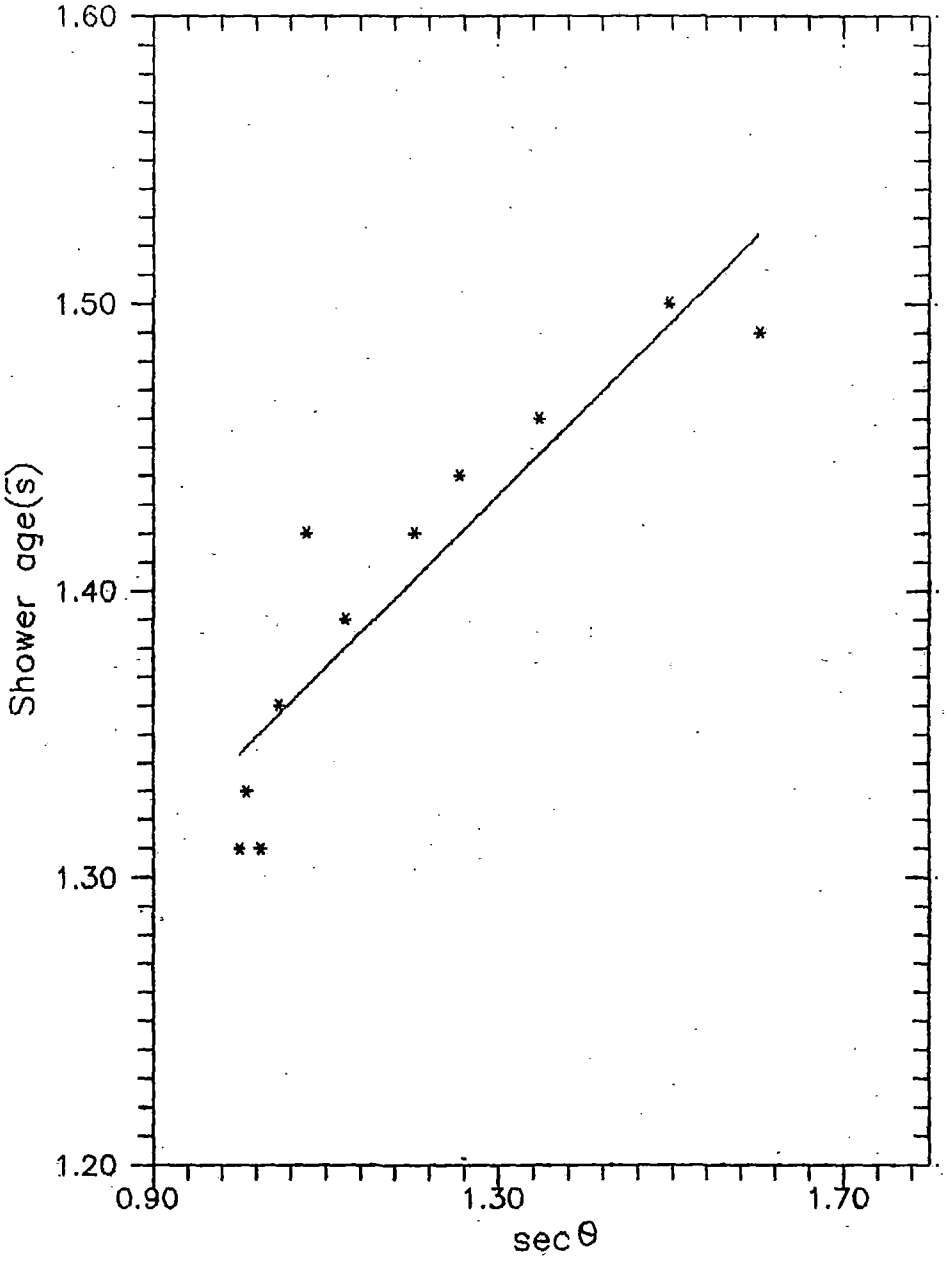

Fig.4.2j.
Variation of shower age with zenith angle for the shower size range $1.5X10^5-5X10^5$

different shower size ranges through the relation as given in equation (4.13), the values of s_o and A for different N_e are also given in table-5.

Table-5 : Comparison of the observed variation of age parameter with zenith angle with the cascade theory for three different shower sizes.

Table-5

	N_e	$6.5X10^4$	$1.2X10^5$	$3.3X10^5$
Observed	s_o	1.19	1.15	1.04
	A	0.24	0.27	0.30
Theory	s_o	1.24	1.20	1.09
	A	0.26	0.28	0.32

From the figs.(fig.4.2h, 4.2i, 4.2j) it is seen that as secθ increases , shower age also increases.Thus with the increase of atmospheric depth (t.secθ), shower age increases. This result shows that the observed variation is in accordance with the electron-photon cascade theory.

4.2.3. **Local age parameter (LAP) :**

At the level of observation of showers, the electron density distribution showing a fit to an effective age (s) parameter results from the superposition of a number of local young and old photon-electron cascades having individual local age parameter [s(r)]. s(r) has been defined in the following way.

Using Hillas structure function and assuming that the normalisation constant does not vary much between two neighbouring radial points r_i, r_j, $s_{ij}(r)$ is obtained (Sanyal S. et al.[26]) as-

$$s_{ij}(r) = \ln (F_{ij} \cdot X_{ij}^{2.07} \cdot Y_{ij}^{3.39}) / 1.54.\ln X_{ij} \quad \text{.....(4.15)}$$

where $F_{ij} = f(r_i) / f(r_j)$, $X_{ij} = r_i / r_j$, $Y_{ij} = (1 + X_i) / (1 + X_j)$ with $X_i = r_i/r_0$ (r_0 = Moliere unit of length) and f(r) = Hillas function

if $r_i \rightarrow r_j$, $s_{ij} \rightarrow s(r)$ where $r = (r_i+r_j)/2$

Substituting the measured electron densities of the showers in the size range 10^6 - $10^{6.2}$ particles at the radial points r_i and r_j in the above equation , LAP at the different radial distances is obtained. Fig.4.2k shows the variation of LAP with radial distances in the present experiment along with the experimental result of Akeno group (Hara T. et al.[27]) and the simulation result of Capdevielle (Capdevielle and Gawin[28]). It is seen from the experimental results that the LAP decreases as core distance increases and reaches minimum around at 32m beyond which it increases again. This variation is similar to that observed in the Akeno experiment.

A general behaviour of s(r) is found to be of the form-

$$s(r) = \alpha\xi^2 + \beta\xi + \gamma \quad \text{.....(4.16)}$$

where $\xi = \ln(r/r_0)$ and α , β , γ are the polynomial coefficients.

There is an agreement with the trend of results of Akeno group and Capdevielle. Table-6 shows the values of the polynomial coefficients of equation (4.16) determined for the present experiment, Akeno experiment and the simulation results of Capdevielle. The present values of the coefficients are satisfactory agreement with the others.

Table-6

Value of the coefficients	Present Expt.	Akeno Expt. with 50mm scintillator.	Simulation of Capdevielle

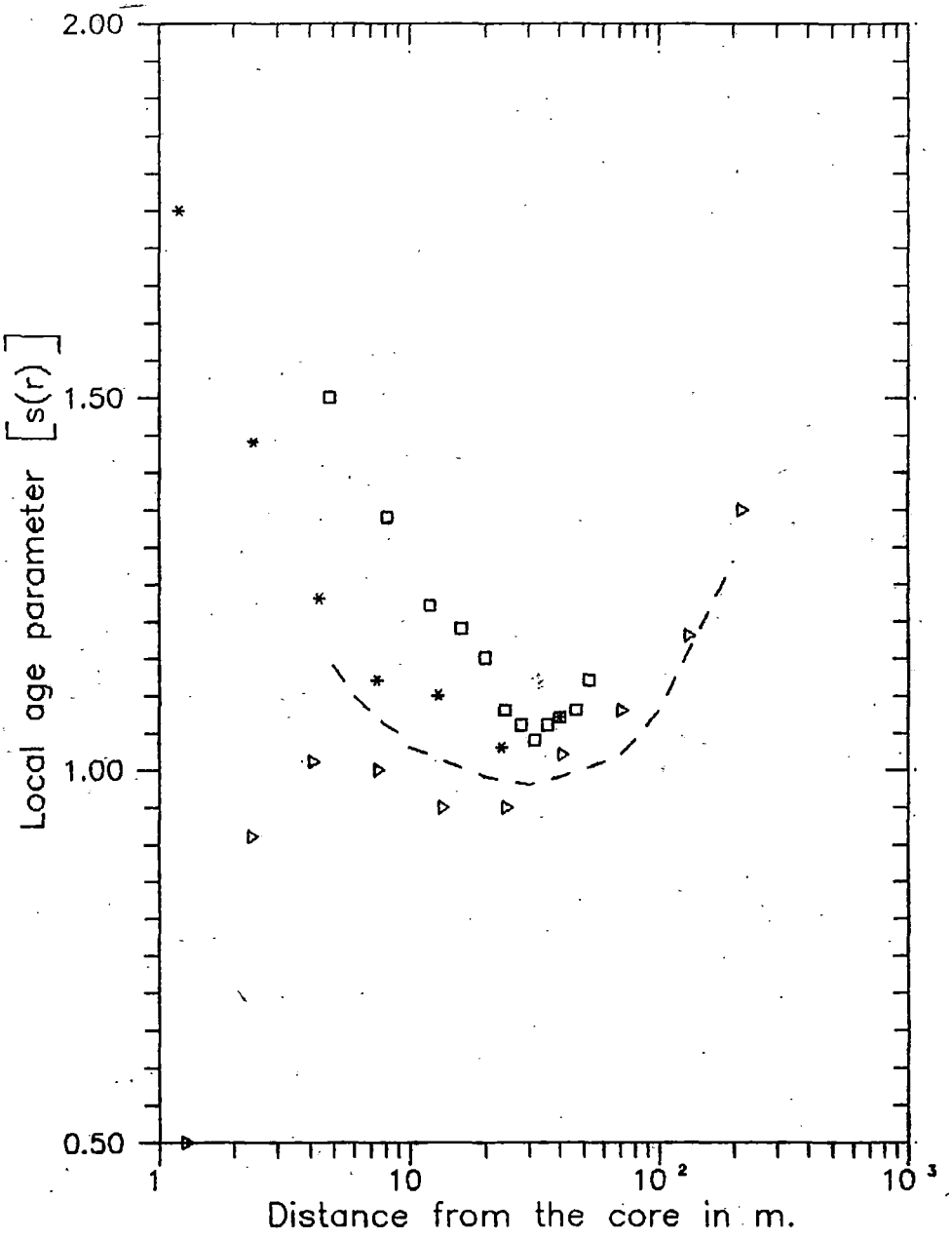

Fig.4.2k.
Variation of local age parameter with core distance.
□..... Present expt.
*..... Akeno with 50mm scintillator.
▷..... Akeno with 3mm scintillator.
dashed line ... Capdevielle et. al.

α	0.099	0.086	0.068
β	0.135	0.229	0.153
γ	1.120	1.192	1.053

Table-6: Values of the polynomial coefficients.

Thus from the experiment it is observed that , the difference between the local age parameter (or lateral age) at the minimum and the observed mean age (longitudinal age) is 0.35.